

Journal Pre-proof

Identification of Novel Quinoline Analogues Bearing Thiazolidinones as Potent Kinase Inhibitors for the Treatment of Colorectal Cancer

Yuting Zhou, Xingwei Xu, Fei Wang, Huan He, Guowei Gong, Li Xiong, Baohui Qi



PII: S0223-5234(20)30615-2

DOI: <https://doi.org/10.1016/j.ejmech.2020.112643>

Reference: EJMECH 112643

To appear in: *European Journal of Medicinal Chemistry*

Received Date: 12 May 2020

Revised Date: 30 June 2020

Accepted Date: 1 July 2020

Please cite this article as: Y. Zhou, X. Xu, F. Wang, H. He, G. Gong, L. Xiong, B. Qi, Identification of Novel Quinoline Analogues Bearing Thiazolidinones as Potent Kinase Inhibitors for the Treatment of Colorectal Cancer, *European Journal of Medicinal Chemistry*, <https://doi.org/10.1016/j.ejmech.2020.112643>.

This is a PDF file of an article that has undergone enhancements after acceptance, such as the addition of a cover page and metadata, and formatting for readability, but it is not yet the definitive version of record. This version will undergo additional copyediting, typesetting and review before it is published in its final form, but we are providing this version to give early visibility of the article. Please note that, during the production process, errors may be discovered which could affect the content, and all legal disclaimers that apply to the journal pertain.

© 2020 Elsevier Masson SAS. All rights reserved.

Identification of Novel Quinoline Analogues Bearing Thiazolidinones as Potent Kinase Inhibitors for the Treatment of Colorectal Cancer

Yuting Zhou, Xingwei Xu, Fei Wang, Huan He, Guowei Gong, Li Xiong, Baohui Qi^{*1}

Department of Bioengineering, Zhuhai Campus of Zunyi Medical University, Zhuhai, 519041, Guangdong Province, China

Abstract:

In this investigation, a novel series of quinoline analogues bearing thiazolidinones were designed and synthesized based on our previous study. Among them, the most potent compound **11k**, 4-((4-(4-(3-(2-(2,6-difluorophenyl)-4-oxothiazolidin-3-yl)ureido)phenoxy)-6-methoxyquinolin-7-yl)oxy)-*N*-isopropylpiperidine-1-carboxamide, possessed submicromolar *c*-Met and Ron inhibitory activities. In addition, enzymatic assays against a mini-panel of kinases (*c*-Kit, B-Raf, *c*-Src, IGF1R, PDGFR α and AXL) were performed, the results showed that compound **11k** exhibited moderate inhibitory activity against PDGFR α , *c*-Src and AXL. MTT assay revealed *in vitro* antitumor activities against HT-29 cells of compound **11k** with an IC₅₀ value of 0.31 μ M which was 9.3- and 34.2-fold more potent than that of Regorafenib (IC₅₀=2.87 μ M) and Cabozantinib (IC₅₀=10.6 μ M). Preliminary antitumor mechanisms were also investigated by cellular assays. Considerable cytotoxicity, antiproliferation and induction of apoptosis of compound **11k** in a dose- and time-dependent manner were confirmed by IncuCyte live-cell imaging assays. Treatment with compound **11k** caused slight G2- or M-phase arrest in HT-29 cells. Further cell selectivity of compound **11k** showed that it was not active against human normal colorectal mucosa epithelial cell FHC at 10.0 μ g/mL. The above results support further structural modification of compound **11k** to improve its inhibitory activity, which will lead to more potent anticancer agents.

Keywords: Anticancer; Tyrosine Kinase; Inhibitors; Quinoline; 1, 3-Thiazolidin-4-one

1. Introduction

Numerous study indicated that receptor and non-receptor protein kinases played an important role in malignant tumor development and progression [1, 2]. Thus, the discovery of drugs targeting receptor or non-receptor protein kinases has comprised a substantial proportion of pharmaceutical research over the past two decades in worldwide. Among the 58 receptor tyrosine kinases, *c*-Met (Mesenchymal-epithelial transition factor) and Ron (Récepteur d'Origine Nantais) has drawn significant attention for their ability of the oncogenic forms to confer growth advantage,

*Corresponding authors.
E-mail address: bhqi@zmu.gd.cn.

protection from apoptosis, invasive properties, and resistance to chemotherapies [3-6].

c-Met, also known as hepatocyte growth factor receptor (HGFR), is a critical member of receptor tyrosine kinase. The c-Met/HGF recruits numerous transduction proteins and triggers its downstream signaling pathways, including phosphoinositide 3-kinase/threonine-protein kinase (PI3K/AKT) axis, mitogen-activated protein kinase (MAPK) cascades, Rac1-Cdc42 and STAT pathways, *etc* [6, 7]. Overexpression and mutation of c-Met is implicated in multiple tumor oncogenic processes, such as tumorigenesis, metastasis, poor prognosis, angiogenesis, invasive growth, and drug resistance [8-10].

Ron, also known as human macrophage stimulating 1 receptor (MST1R), is the only other member of c-Met family. The structures of the two kinases are very similar, and they share 34% overall homology and the tyrosine kinase region of the receptors share 80% homology [11, 12]. RON gene is rarely or not expressed in normal epithelial tissue, while in bladder, lung, thyroid, colon, skin, breast and pancreas tumors it is highly expressed and is usually accompanied by the generation of variants [13]. The phosphorylated Ron can activate a great number of transduction proteins and trigger its downstream signaling cascades, including c-Src, β -catenin/TCF-4, ERK1/2, MAPK, SMAD/TGF- β , JNK/STAT, and PI3K/AKT, *etc* [14-16]. The dysregulation of Ron has shown to be associated extensively with the process of the induction and development of tumorigenesis, such as cell proliferation, migration, invasion, survival, angiogenesis, epithelial-to-mesenchymal transition (EMT) and drug resistance [17, 18].

Over expression and/or aberrant activation of c-Met and Ron in different kinds of cancers suggested that they were important targets for cancer therapy. In the past decades, there has been a flourish of activity to develop small molecule c-Met and/or Ron kinase inhibitors, and a number of structurally diverse inhibitors have been reported, such as BMS777607, Crizotinib, Cabozantinib, MK-8033, Capmatinib and Merestinib (Fig. 1) [19-25]. However, the majority of studies have been limited to *in vitro* experiments due to unfavorable pharmacologic and/or pharmacokinetic properties, as well as intolerable toxicity. Based on our previous study, we report the identification of novel quinoline analogues bearing thiazolidinones as potent inhibitors of c-Met and Ron kinases, as well as their antitumor activity and antitumor mechanism. In addition, the structure-activity relationship (SAR) and docking studies are also presented in the present work.

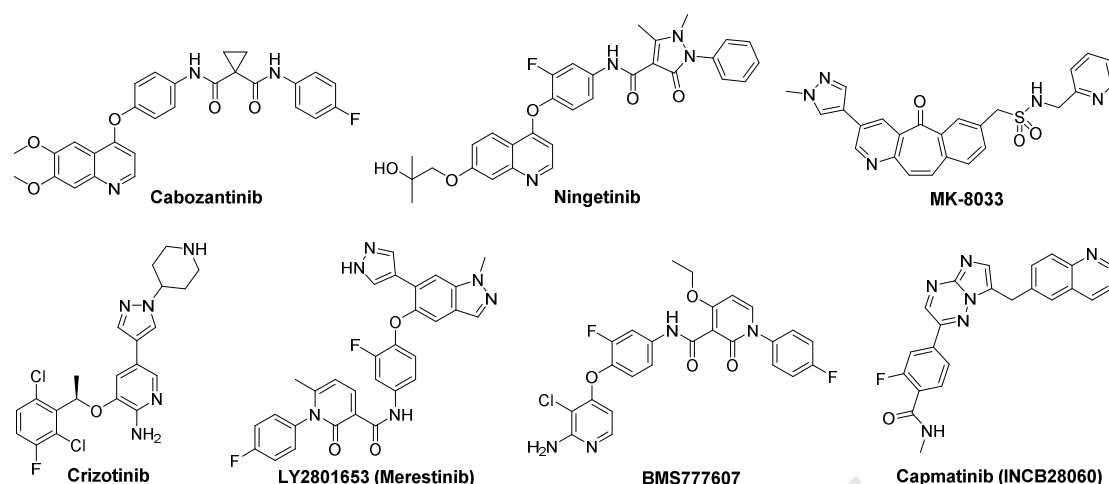


Fig. 1 The representative c-Met and/or Ron inhibitors.

2. The design of novel compounds

We previously disclosed a multi-tyrosine kinase inhibitor, N^1 -(4-((7-(3-(4-ethylpiperazin-1-yl)propoxy)-6-methoxyquinolin-4-yl)oxy)-3,5-difluorophenyl)- N^3 -(2-(2,6-difluorophenyl)-4-oxothiazolidin-3-yl)urea, which showed IC_{50} values of 15.0 nM and 2.9 nM against c-Met and Ron, respectively (Fig. 2) [26]. The results of SARs indicated: (1) the terminal heterocycles of part I reached out into the solvent, and it was a potential position to improve the anticancer activity and the aqueous solubility (Fig. 2 and Fig. 3C); (2) a phenyl ring substituted by fluorine atom in Part II was well tolerated; (3) the nitrogen atom of quinoline form a strong H-bond with Met1160 (Fig. 3B) [26].

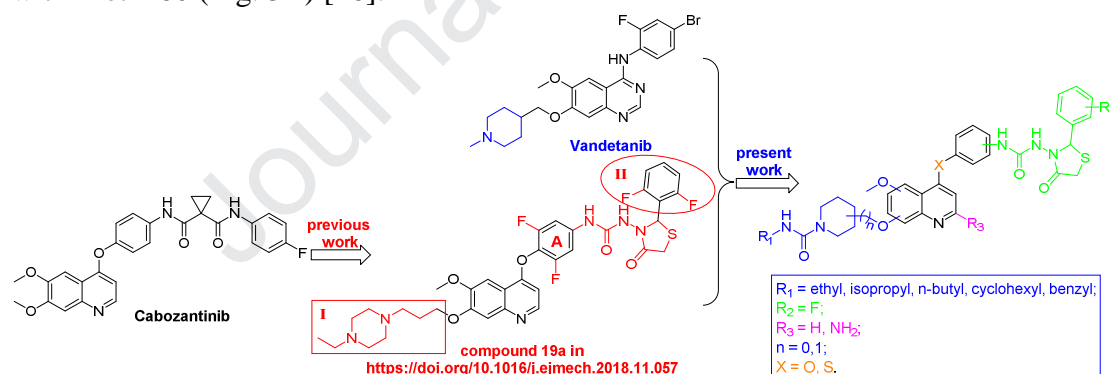


Fig. 2 Our previous work and the design of novel compounds in the present work.

According to the structure of Vandetanib, we first modified the structure of the compound obtained in our previous work by replacing of the (4-ethylpiperazin-1-yl)propoxy group (part I) with substituted piperidine-1-carboxamide, a fragment bearing hydrophilic groups (Fig. 2). The best position and the number of fluorine atoms were further investigated in the following modification of part II. Subsequently, some compounds were synthesized by changing the linker atom (O or S) between phenyl ring A and quinoline and the position (3- or 4-) of thiazolidinone urea attached to the phenyl ring A.

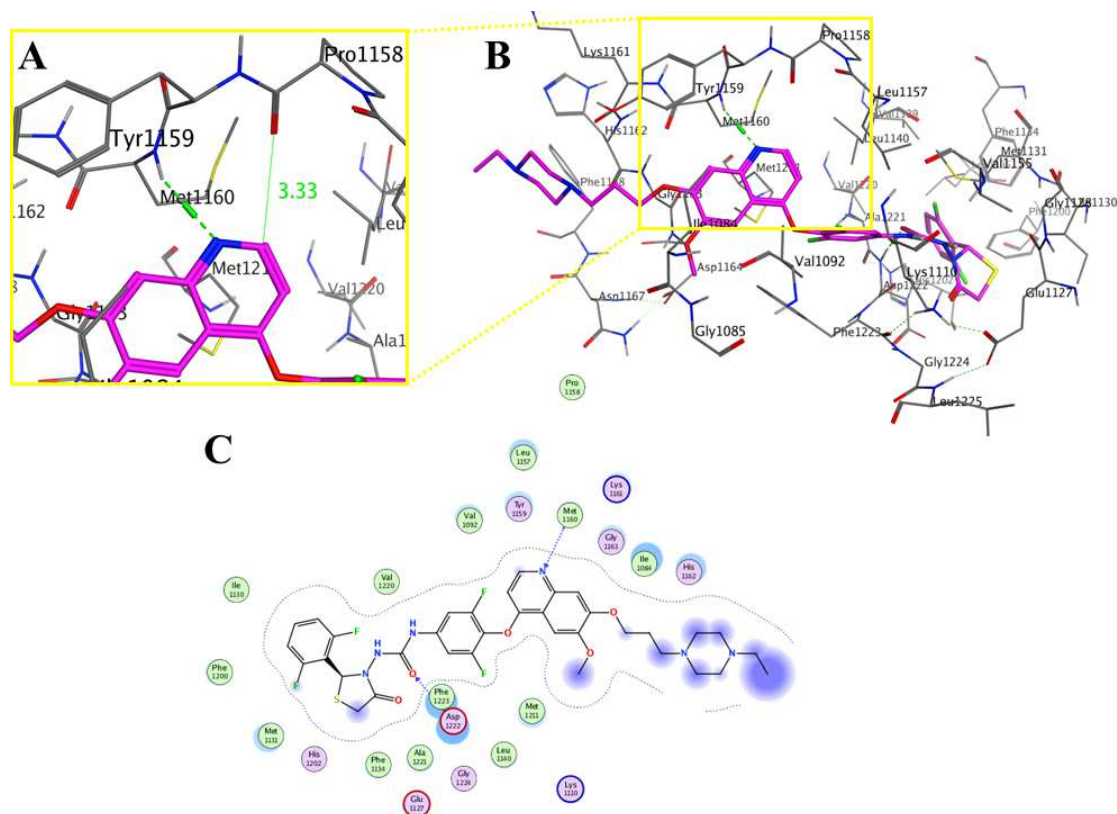


Fig. 3 The binding mode of compound obtained in our previous work with c-Met kinase (PDB ID: 3LQ8). The H-bonds were represented by green dotted lines.

Docking study showed that the distance between the oxygen in carbonyl group of Pro1158 and the carbon at the 2-position of quinoline ring was 3.33 Å (Fig. 3A). Thus, an additional H-bond might be formed by introducing a H-bond donor at the 2-position of quinoline. Hence, a 2-aminoquinoline derivative was designed and synthesized in the present work.

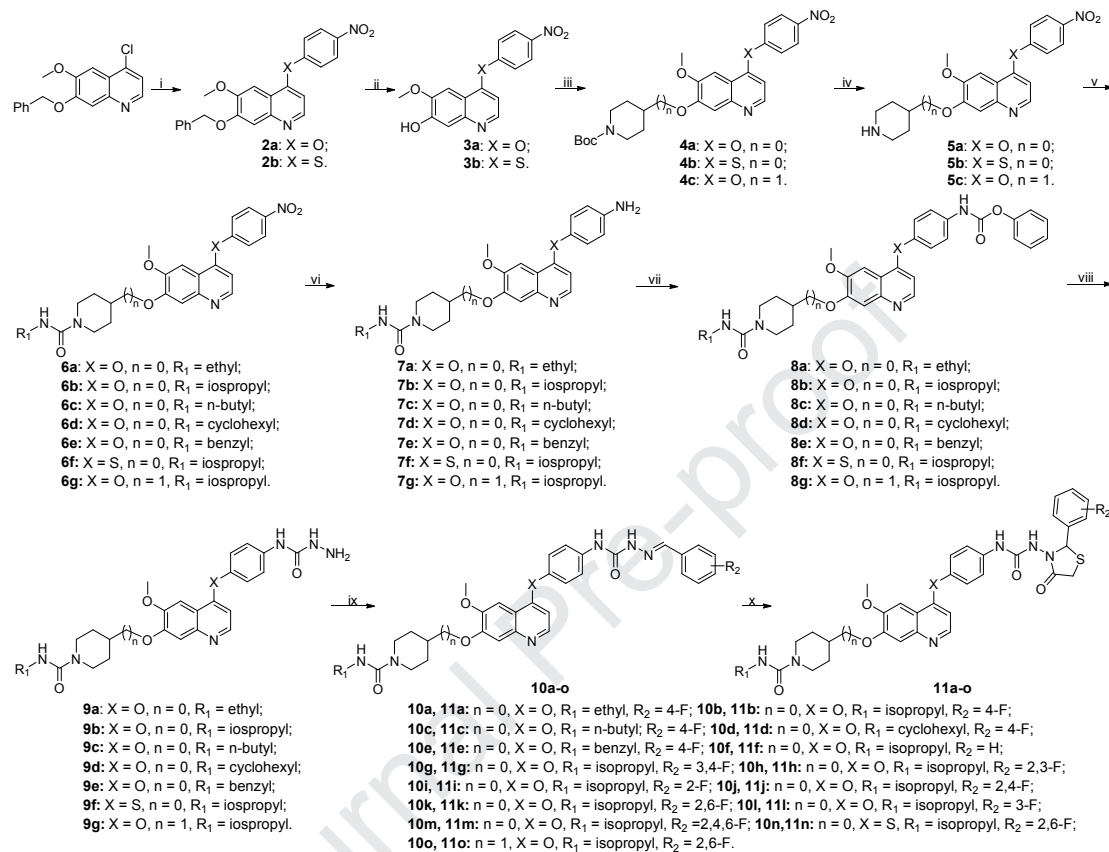
Based on the above assumption, totally nineteen compounds were designed, prepared, and evaluated for their biological activity in the present work.

3. Results and Discussion

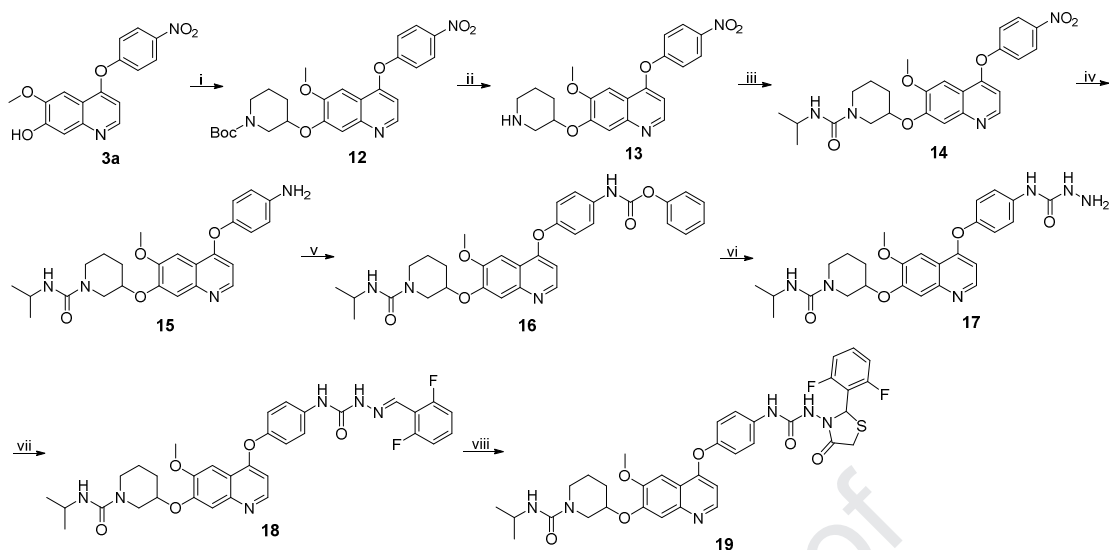
3.1. Chemistry

All newly compounds were prepared by synthetic routes outlined in Schemes 1-5. Scheme 1 showed the synthetic routes for target compounds **11a-o**. Starting from commercially available 7-(benzyloxy)-4-chloro-6-methoxyquinoline, substitution of chloride with 4-nitrophenol or 4-nitrothiophenol gave nitro **2a-b**, which were converted to phenols **3a-b** in the presence of HBr [27]. Reaction of **3a-b** with 1-Boc-4-methanesulfonyloxypiperidine or 1-Boc-4-(((methylsulfonyl)oxy)methyl)piperidine in DMF containing Cs_2CO_3 provided ethers **4a-c** [28]. Piperidines **5a-c** were obtained by clean deprotection of the *N*-Boc group using CF_3COOH in CH_2Cl_2 . Treatment of **5a-c** with different isocyanates gave intermediates **6a-g**, which were reduced by powdered iron in 90% EtOH to afford amines **7a-g**. To obtain semicarbazides **9a-g**, the amines **7a-g** were reacted with phenyl chloroformate in the presence of pyridine to afford **8a-g**, followed by hydrazinolysis reaction with 80% hydrazine hydrate in xylene with vigorous

agitation. Condensation of **9a-g** with different benzaldehydes was carried out to yield semicarbazones **10a-o** in favor of catalytic HOAc in *i*-PrOH. Finally, target compounds **11a-o** were obtained via the cyclization with mercaptoacetic acid under SiCl₄ in dry CH₂Cl₂. Taking intermediate **3a** as starting material, target compound **19** was prepared by similar synthetic routes outlined in Scheme 2.

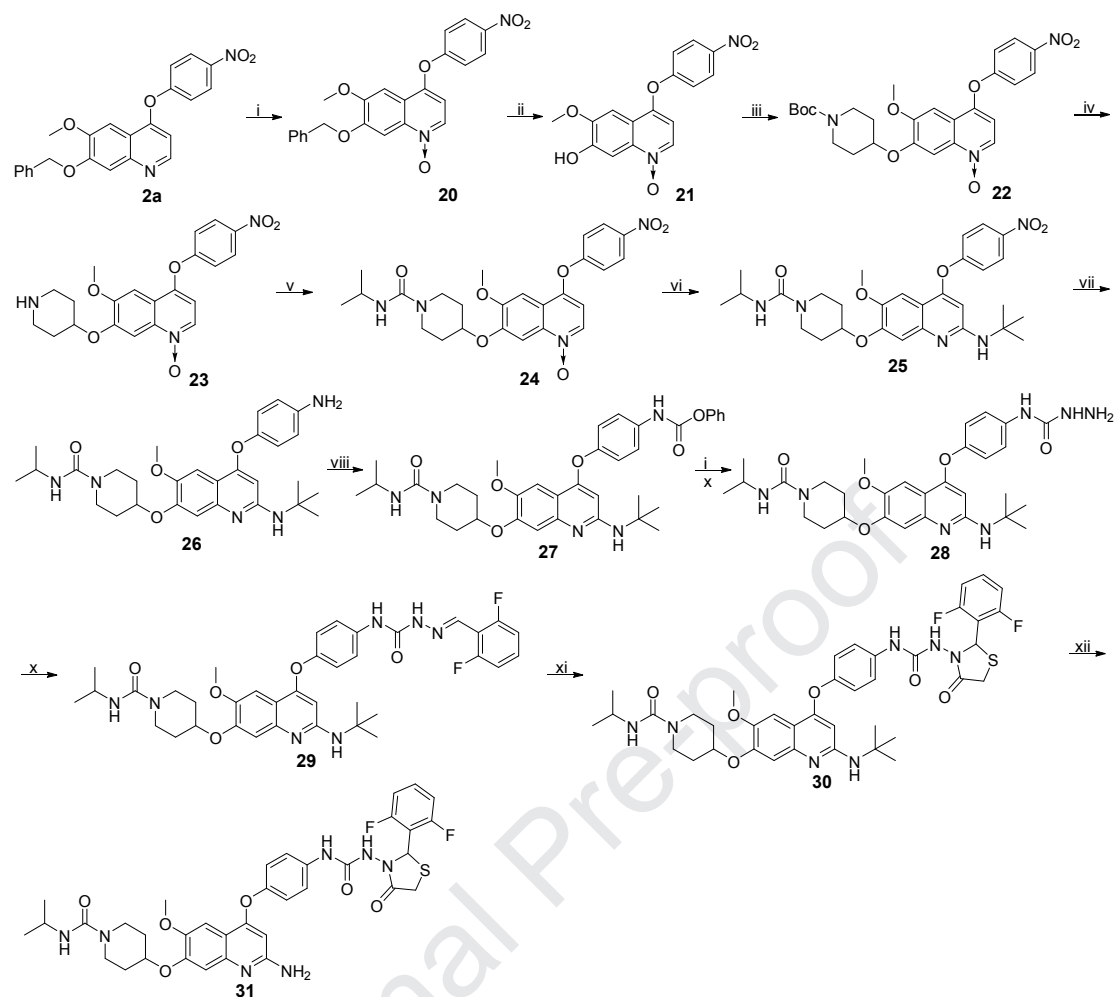


Scheme 1. Synthesis of target compounds **11a-o**. Reagents and conditions: i) 4-nitrophenol (**2a**) or 4-nitrothiophenol (**2b**), PhCl, reflux, 16 h, 60.1-62.4%; ii) 33% HBr in HOAc, rt, 3 h, 64.2-66.4%; iii) 1-Boc-4-methanesulfonyloxypiperidine or 1-Boc-4-(((methylsulfonyl)oxy)methyl)piperidine, Cs₂CO₃, DMF, 110 °C, 6 h, 46.7-55.3%; iv) CF₃COOH, CH₂Cl₂, rt, 2 h, 74.8-79.6%; v) isocyanates, Et₃N, CH₂Cl₂, rt, 3-5 h, 76.4-84.2%; vi) Fe, 90% EtOH, HCl, reflux, 4-6 h, 77.4-85.8%; vii) phenyl chloroformate, pyridine, CH₂Cl₂, rt, 2 h; viii) 80% hydrazine hydrate, xylene, 70 °C, 2 h, 31.9-41.5%; ix) aldehydes, *i*-PrOH, HOAc (cat.), reflux, 2 h, 77.7-86.1%; x) mercaptoacetic acid, SiCl₄, CH₂Cl₂, reflux, 6 h, 36.3-45.8%.



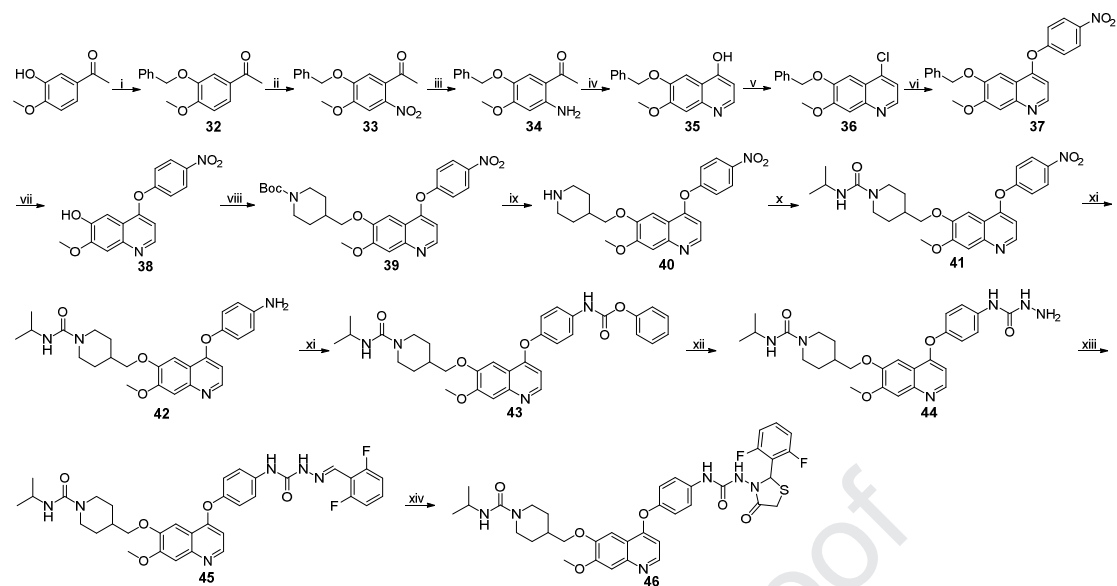
Scheme 2. Synthesis of target compound **19**. Reagents and conditions: i) 1-Boc-3-methanesulfonyloxypiperidine, Cs_2CO_3 , DMF, 110°C , 6 h, 39.8%; ii) CF_3COOH , CH_2Cl_2 , rt, 2 h, 73.2%; iii) isopropyl isocyanate, Et_3N , CH_2Cl_2 , rt, 3 h, 79.3%; iv) Fe, 90% EtOH, HCl, reflux, 6 h, 81.6%; v) phenyl chloroformate, pyridine, CH_2Cl_2 , rt, 2 h; vi) 80% hydrazine hydrate, xylene, 70°C , 2 h, 34.2%; vii) 2,6-difluorobenzaldehyde, *i*-PrOH, HOAc (cat.), reflux, 2 h, 81.9%; viii) mercaptoacetic acid, SiCl_4 , CH_2Cl_2 , reflux, 6 h, 39.6%.

The synthesis of compound **31** was accomplished in a multiple process as shown in Scheme 3. Intermediate **2a** was cleanly oxidated by *m*-CPBA in CH_2Cl_2 to afford quinoline *N*-oxide **20** [29]. Intermediate **24** was obtained via debenzylation, nucleophilic substitution, deprotection of the *N*-Boc group and amination reaction by similar synthetic methods preparing intermediate **6**. Quinolines *N*-oxide **24** were readily converted to 2-*tert*-butylaminoquinoline **25** by Ts_2O and *t*- BuNH_2 in CH_2Cl_2 [30]. In the following steps, intermediate **30** were synthesized using a method similar to that for compounds **11a-o**. Finally, the deprotection of *t*-butyl group was achieved by stirring at 70°C in the presence of CF_3COOH in xylene.



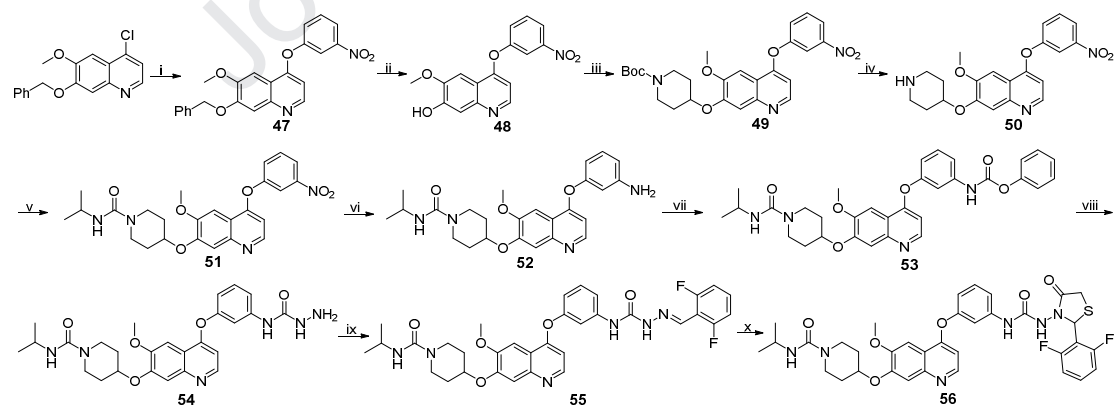
Scheme 3. Synthesis of compounds **31**. Reagents and conditions: i) *m*-CPBA, CH₂Cl₂, rt, 67.7%; ii) 33% HBr in HOAc, rt, 3 h, 65.1%; iii) 1-Boc-4-methanesulfonyloxypiperidine, Cs₂CO₃, DMF, 110 °C, 6 h, 49.3%; iv) CF₃COOH, CH₂Cl₂, rt, 2 h, 78.5%; v) isopropyl isocyanate, Et₃N, CH₂Cl₂, rt, 3 h, 74.3%; vi) *t*-BuNH₂, Ts₂O, CH₂Cl₂, rt, 1 h, 62.1%; vii) Fe, 90% EtOH, HCl, reflux, 6 h, 76.2%; viii) phenyl chloroformate, pyridine, CH₂Cl₂, rt, 2 h; ix) 80% hydrazine hydrate, xylene, 70 °C, 2 h, 38.6%; x) 2,6-difluorobenzaldehyde, *i*-PrOH, HOAc (cat.), reflux, 2 h, 78.4%; xi) mercaptoacetic acid, SiCl₄, CH₂Cl₂, reflux, 6 h, 41.0%; xii) CF₃COOH, xylene, 70 °C, 5 h, 57.9%.

Scheme 4 presents the synthetic routes for target compound **46**. Commercially available 1-(3-hydroxy-4-methoxyphenyl)ethan-1-one was reacted with benzyl bromide under basic condition in DMF to afford **32**. Nitration of **32** with fuming nitric acid in CH₂Cl₂ afforded nitro **33**, which was then reduced by powdered iron to give amine **33** in satisfactory yield [31]. Cyclization was accomplished in the presence of MeONa and HCOOEt to yield quinoline **35** [32]. The resultant hydroxyl moiety **35** were converted to the corresponding chloride **36** on exposure to phosphorus oxychloride in the presence of 4-dimethylaminopyridine. Subsequently, compound **46** was obtained using a method similar to that for compound **11o** via S_N2 nucleophilic substitution, debenylation, deprotection of the *N*-Boc group, amination, reduction, acylation, hydrazinolysis, condensation and cyclization reaction.



Scheme 4. Synthesis of target compound **46**. Reagents and conditions: i) benzyl bromide, K_2CO_3 , DMF, rt, 2 h, 89.8%; ii) fuming HNO_3 , $-10^\circ C$, 5 h, 73.6%; iii) Fe, 90% EtOH, HCl, reflux, 3 h, 78.5%; iv) MeONa, HCOOEt, DME, rt, 4 h, 72.4%; v) 4-dimethylaminopyridine, $POCl_3$, $110^\circ C$, 6 h, 64.7%; vi) 4-nitrophenol, PhCl, reflux, 16 h, 58.6%; vii) 33% HBr in HOAc, rt, 3 h, 63.8%; viii) 1-Boc-4-(((methylsulfonyl)oxy)methyl)piperidine, CS_2CO_3 , DMF, $110^\circ C$, 6 h, 47.3%; ix) CF_3COOH , CH_2Cl_2 , rt, 2 h, 74.4%; x) isopropyl isocyanate, Et_3N , CH_2Cl_2 , rt, 3 h, 81.2%; xi) phenyl chloroformate, pyridine, CH_2Cl_2 , rt, 2 h; xii) 80% hydrazine hydrate, xylene, $70^\circ C$, 2 h, 39.7%; xiii) aldehydes, *i*-PrOH, HOAc (cat.), reflux, 2 h, 83.1%; xiv) mercaptoacetic acid, $SiCl_4$, CH_2Cl_2 , reflux, 6 h, 37.2%.

Synthetic routes for target compound **56** are displayed in Scheme 5. Commercially available 7-(benzyloxy)-4-chloro-6-methoxyquinoline and 3-nitrophenol were converted to target compound **56** via a series of similar reactions as described above.



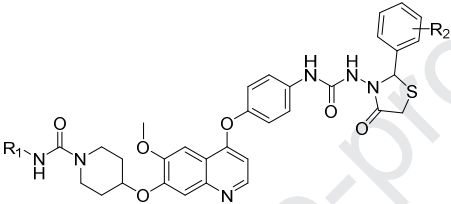
Scheme 5. Synthesis of target compound **56**. Reagents and conditions: i) 3-nitrophenol, PhCl, reflux, 16 h, 52.4%; ii) 33% HBr in HOAc, rt, 3 h, 62.0%; iii) 1-Boc-4-methanesulfonyloxypiperidine, CS_2CO_3 , DMF, $110^\circ C$, 6 h, 51.2%; iv) CF_3COOH , CH_2Cl_2 , rt, 2 h, 80.2%; v) isopropyl isocyanate, Et_3N , CH_2Cl_2 , rt, 3 h, 76.5%; vi) Fe, 90% EtOH, HCl, reflux, 4 h, 81.2%; vii) phenyl chloroformate, pyridine, CH_2Cl_2 , rt, 2 h; viii) 80% hydrazine hydrate, xylene, $70^\circ C$, 2 h, 40.3%; ix) 2,6-difluorobenzaldehyde, *i*-PrOH, HOAc (cat.), reflux, 2 h, 76.9%; x) mercaptoacetic acid, $SiCl_4$, CH_2Cl_2 , reflux, 6 h, 35.2%.

3.2. Results and discussion

3.2.1. Structure-Activity Relationship

In our previous study, we found that the quinoline derivatives bearing thiazolidinone fragments showed potent *in vitro* kinase inhibitory activity against c-Met/Ron and anticancer activity against various cancer cell lines, especially human colorectal cancer cell line HT-29 [26]. Moreover, c-Met and Ron overexpression is correlated with colorectal cancer (CRC) and CRC liver metastasis [33-35]. Thus, *in vitro* anticancer activity of all newly synthesized compounds against HT-29 cells was determined in the present study. Due to the weak antitumor activity of Cabozantinib against HT-29 cells, Regorafenib treatment for metastatic colorectal cancer (mCRC) in clinic was chosen as another positive control. The inhibitory potencies against c-Met, Ron and HT-29 cells were shown in Table 1 and Table 2.

Table 1. *In vitro* kinase inhibitory activity and anticancer activity of compounds **11a-m**.



Compd.	R ₁	R ₂	Inhibitory activities		IC ₅₀ (μM) ^c		HT-29 IC ₅₀ (μM) ^d
			c-Met ^a	Ron ^b	c-Met	Ron	
11a		4-F	23.6	25.9	ND ^c	ND	2.25 ± 0.25
11b		4-F	29.1	33.7	ND	ND	0.86 ± 0.072
11c		4-F	14.4	19.9	ND	ND	1.70 ± 0.18
11d		4-F	24.4	26.2	ND	ND	3.42 ± 0.21
11e		4-F	3.5	4.1	ND	ND	6.60 ± 0.46
11f		H	31.2	50.6	1.68	0.503	1.26 ± 0.11
11g		3,4-F	16.1	21.2	ND	ND	1.06 ± 0.085
11h		2,3-F	19.5	31.1	ND	ND	0.79 ± 0.057
11i		2-F	41.1	60.3	0.531	0.347	0.41 ± 0.034
11j		2,4-F	19.8	33.8	ND	ND	0.95 ± 0.086
11k		2,6-F	65.0	84.4	0.382	0.122	0.31 ± 0.022
11l		3-F	22.5	26.8	ND	ND	0.67 ± 0.058
11m		2,4,6-F	31.2	37.5	ND	ND	0.91 ± 0.079
Regorafenib	-	-	ND	ND	ND	ND	2.87 ± 0.19
Cabozantinib	-	-	98.6	75.2	ND	ND	10.6 ± 1.12

^a The kinase inhibition % at 1.0 μM are the average of two independent experiments.

^b The kinase inhibition % at 0.5 μM are the average of two independent experiments.

^c The IC₅₀ values are the average of two independent experiments.

^d The values were an average of three separate determinations and standard deviations were shown.

^e ND: Not determined.

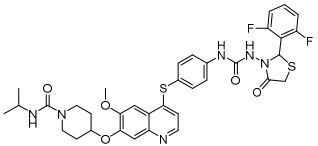
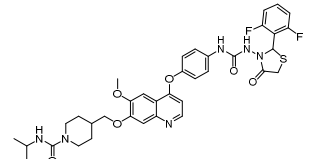
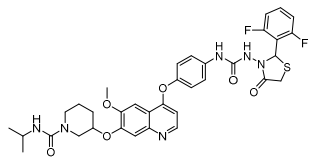
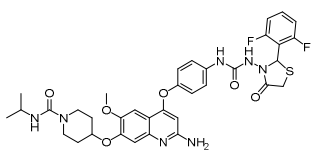
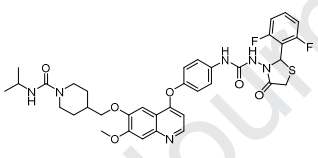
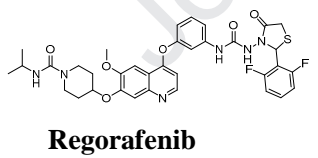
To examine the substitution effect of R₁ in the piperidine urea moiety (Fig. 2), various substituents were introduced, including benzyl group, isopropyl group and ethyl group, *etc* (**11a-e**). According to the biological results, isopropyl group (**11b**) was fixed as the optimal group. Comparing the inhibitory potencies of **11b** to that of

11e, a preliminary conclusion might be made that the introduction of hydrophobic and bulky group at R₁ dramatically decreased the activity against all the two kinases and HT-29 cells, such as benzyl group (**11e**).

In the following modification, our attention turned to the R₂. Based on our previous study, only well tolerated fluorine atoms were introduced. The potency contribution of the *ortho*-fluoro substituent on the phenyl ring was demonstrated by **11i** and **11k** compared to **11f**. The addition of 2,6-difluoro (**11k**) imparted 4.4- and 4.1-fold increase in enzymatic potency (c-Met IC₅₀=0.382 μM and Ron IC₅₀=0.122 μM) and a 4.1-fold increase of cellular potency (IC₅₀=0.31 μM) relative to the **11f** (c-Met IC₅₀=1.68 μM, Ron IC₅₀=0.503 μM and HT-29 IC₅₀=1.26 μM). As a general trend, moving fluorine atom to *meta*- or *para*-position on the phenyl ring resulted in a loss of activity against kinases and cancer cell.

Having identified well tolerated group on R₁ (R₁ = isopropyl group) and R₂ (R₂ = 2, 6-difluoro), we next further explored the SAR, including the linker atom between quinoline and phenyl ring A (**11n**), 2-, 6- and 7-positions on quinoline (**11o**, **19**, **31**, **46**) and the position of thiazolidinone urea moiety linked on phenyl ring A (**56**). As indicated in Table 2, the replacement of the oxygen (**11k**) with a sulfur linker (**11n**) was tolerated except for the activity against HT-29. The introduction of an amino in 2-position of quinoline (**31**) imparted 1.8- and 4-fold decrease in c-Met and Ron kinase inhibitory rate and 18-fold decrease of cell potency. Docking study showed that compound **31** adopted a similar docking mode comparing to that of **11k**, and an additional H-bond was formed between the amino and the residue Pro1158 (Fig. 5B). Unfortunately, the newly formed H-bond interaction was weak (data not shown). In addition, the H-bond between nitrogen atom of quinoline and the residue Met1160 was weakened due to the changes of conformation resulted from the introduction of NH₂. Movement of the thiazolidinone urea moiety from 4- to 3-position on the phenyl ring A led to a dramatically reduced enzymatic potency and cellular potency (**56** vs **11k**). The results of docking study indicated that the loss of a H-bond formed between the oxygen atom in the urea moiety and Lys1110 might lead to the lower potency (Fig. 5D). Finally, the effect of varying the methoxy group and *N*-isopropylpiperidine-1-carboxamide on the quinoline was examined with the ultimate goal to improve inhibitory activity and introduce water solubilizing groups. Compared **11o** with **11k**, a slight drop in enzymatic potency and cellular potency was observed by lengthening the distance between oxygen atom and piperidine ring. Notably, compound **46** bearing the *N*-isopropylpiperidine-1-carboxamide on the 6-position of quinoline displayed over 25-fold lower potency against HT-29 cells (IC₅₀>10.0 μM) than compound **11o**. The results indicated that a substituted piperidine-1-carboxamide at the 7-position of quinoline was necessarily required for kinases and cancer cell inhibition.

Table 2. *In vitro* kinase inhibitory activity and anticancer activity of compounds **11n-o**, **19**, **31**, **46** and **56**.

Compd.	Inhibitory activities		IC ₅₀ (μM) ^c		HT-29 IC ₅₀ (μM) ^d
	c-Met ^a	Ron ^b	c-Met	Ron	
11n 	62.9	83.0	ND ^e	ND	0.42 ± 0.031
11o 	58.4	86.1	ND	ND	0.39 ± 0.028
19 	31.7	39.7	ND	ND	>10.0
31 	34.7	21.1	ND	5.53	5.60
46 	20.7	25.3	ND	ND	>10.0
56 	16.0	29.3	ND	ND	>10.0
Regorafenib	-	-	ND	ND	2.87 ± 0.18
Cabozantinib	98.6	75.2	ND	ND	10.6 ± 1.12

^a The kinase inhibition % at 1.0 μM are the average of two independent experiments.

^b The kinase inhibition % at 0.5 μM are the average of two independent experiments.

^c The IC₅₀ values are the average of two independent experiments.

^d The values were an average of three separate determinations and standard deviations were shown.

^e ND: Not determined.

3.2.2. Molecular docking study

In order to explore the binding mode of this series of compounds and explain the SAR, docking simulation studies of representative compound **11k**, **31** and **56** were performed. As shown in Fig. 4B, 5B, 5D and 6, all compounds adopted an extend conformation as type II kinase inhibitors. The most potent compound **11k** formed three canonical hydrogen bonds with the residues of Lys1110, Met1160 and Lys1161. H-arene interactions were formed by quinoline and 2, 6-difluorophenyl fragment with

Val1092 and Phe1134, respectively. In addition, the *N*-isopropylpiperidine-1-carboxamide was protruded into solvent, and the terminal 2,6-difluorophenyl ring inserted into a hydrophobic pocket formed by the residues of Phe1134, Phe1200 and Ala1221, *etc.*

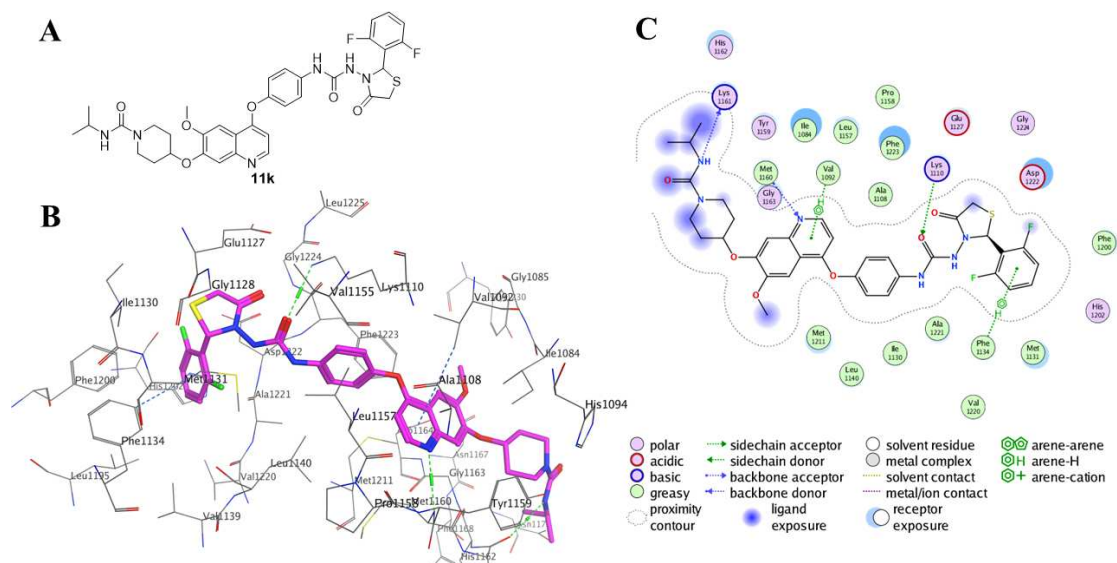


Fig. 4 The proposed binding mode of compound **11k** with c-Met kinase (PBD ID: 3LQ8). A) The structure of compound **11k**. B) The interactions between compound **11k** and c-Met. The compound was shown by purple sticks, the H-bonds were represented by green dotted lines, and the arene-H interaction was shown by blue dotted lines. C) 2D depiction of the ligand-protein interactions.

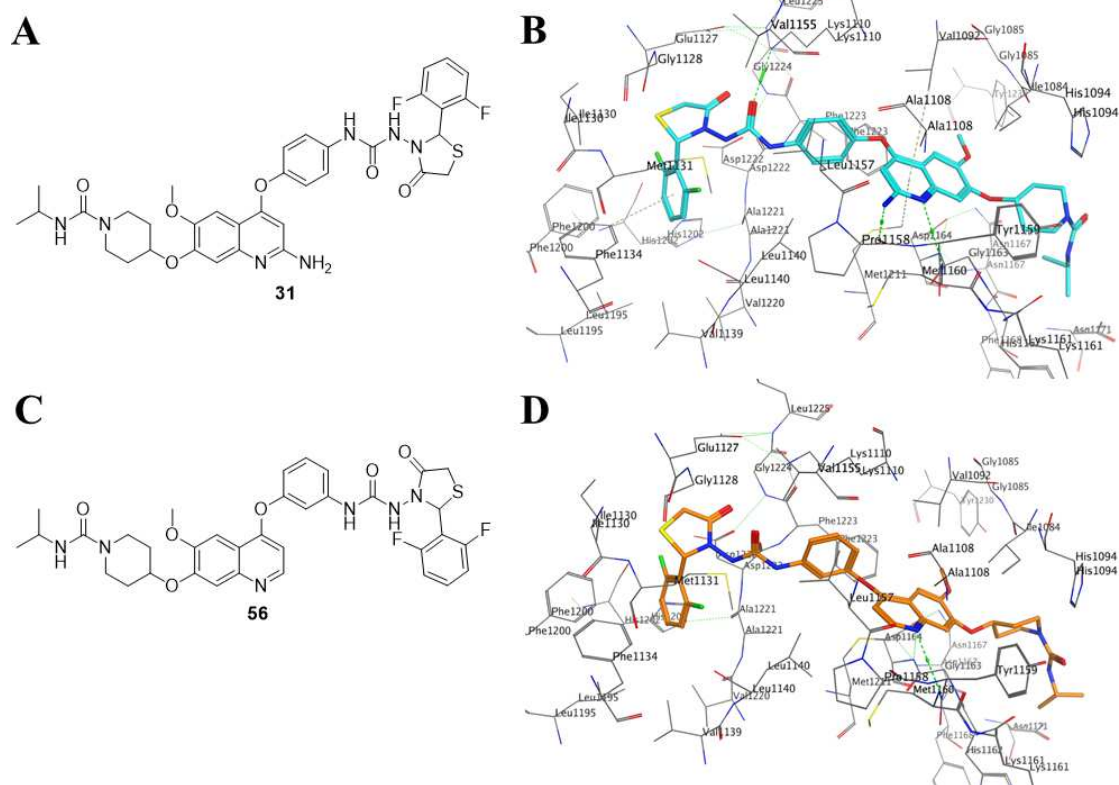


Fig. 5 The proposed binding mode of compounds **31** and **56** with c-Met kinase (PBD ID: 3LQ8). A) The structure of compound **31**. B) The interactions between compound **31** and c-Met. The compound

was shown by blue sticks, and the H-bonds were represented by green dotted lines. C) The structure of compound **56**. D) The interactions between compound **56** and c-Met. The compound was shown by yellow sticks, and the H-bond was represented by green dotted lines.

As depicted in Fig. 6, compounds **11k**, **31** and **56** were well embedded in the binding pocket by similar alignment (Fig. 6). The conformations of three compounds were slightly different which led to different enzymatic, and the details were explained in the section of structure-activity relationship.

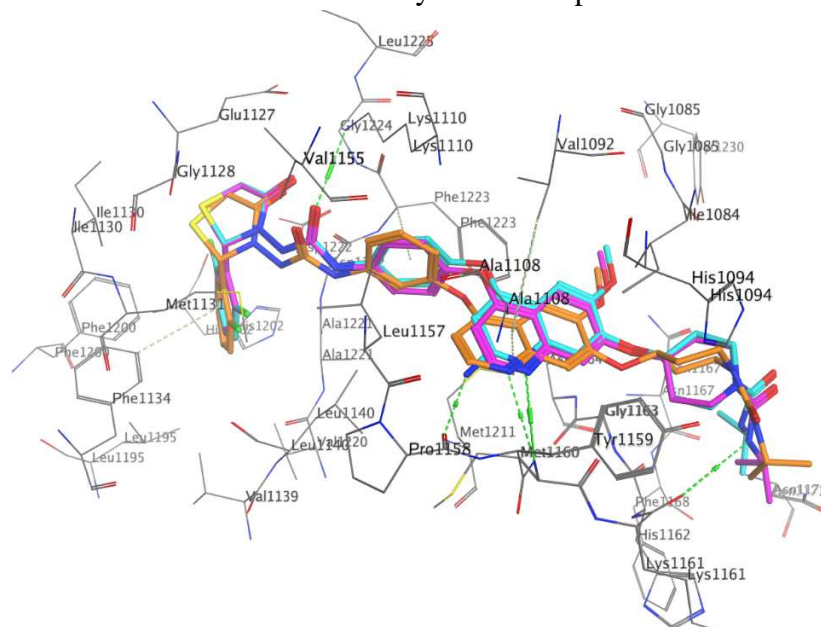


Fig. 6 The superposition of compounds **11k**, **31** and **56**. The compounds **11k**, **31** and **56** were shown by purple, blue and yellow sticks, respectively. The H-bonds were represented by green dotted lines.

3.2.3. IncuCyte live-cell imaging assays

Taking Regorafenib as positive control, antitumor mechanism and cytotoxicity against normal cells of the most potent compound **11k** were illustrated by IncuCyte live-cell imaging assays in the following work.

3.2.3.1. Antiproliferation and cytotoxicity against HT-29

Real-time monitoring the confluence and the number of dead HT-29 cells was performed to compare the effects of compound **11k** and Regorafenib upon the kinetics of antiproliferation and cytotoxicity. As shown in Fig. 7A and 8, a reduction in cell proliferation induced by compound **11k** was observed which was inferior to that of Regorafenib at the same concentration. Exhilaratingly, 5.0 $\mu\text{g/mL}$ of compound **11k** led to a significant cytotoxicity, and no cytotoxicity could be seen by treatment with 5.0 $\mu\text{g/mL}$ of Regorafenib (Fig. 7B and 8). Lower concentration (1.67 $\mu\text{g/mL}$ and 0.56 $\mu\text{g/mL}$) of compound **11k** could also induced strong cytotoxicity, especially after treatment for 36 h. The above results indicated that compound **11k** could induce antiproliferation and cytotoxicity in a dose- and time-dependent manner.

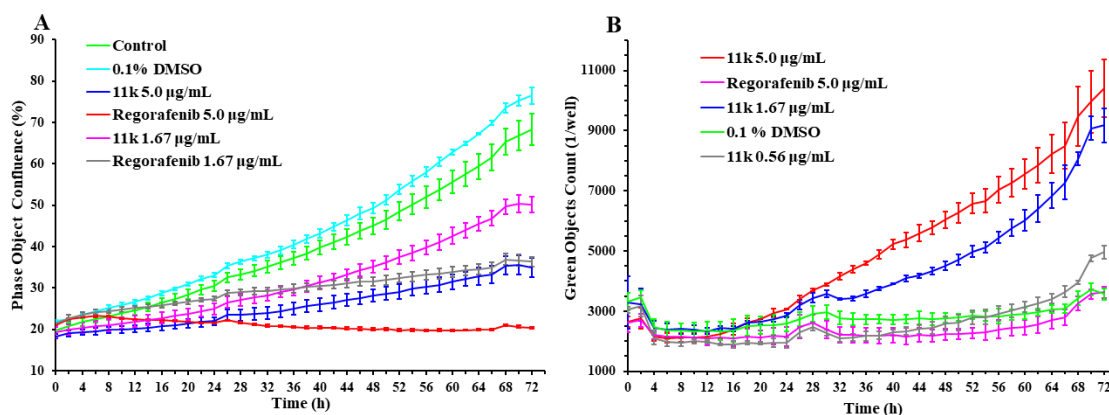


Fig. 7 The curves of InCuCyte live-cell imaging assays in HT-29 cell lines. All error bars are expressed as mean \pm SD of three independent experiments. A) The curves of real-time cell confluence. The cell population was monitored for 72 h using an InCuCyte ZOOM system in an incubator. B) The curves of real-time cytotoxicity. The dead cell population was monitored for 72 h using an InCuCyte ZOOM system in an incubator.

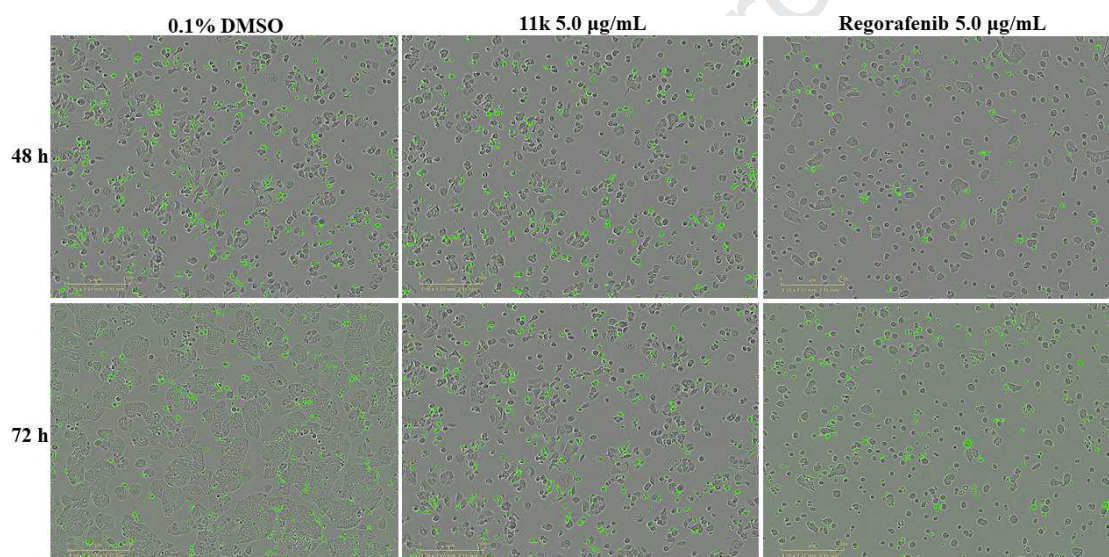


Fig. 8 The white light images (merged) of study on antiproliferation and cytotoxicity against HT-29 cell lines after 48 h and 72 h of treatment with compound **11k**, Regorafenib or 0.1% DMSO. Green fluorescent cells were counted as dead cell. Nucleus were stained with the DNA fluorescent probe YOYO-1 iodide.

3.2.3.2. Measurement of apoptosis

Inducing apoptosis is often considered as one of the major strategies for antitumor-drug development. Thus, in order to characterize the mode of cell death induced by compound **11k**, apoptosis analysis was performed. 3.0 µg/mL of compound **11k** induced significant apoptosis on HT-29 cells after 36 h which was much greater than that of Regorafenib (Fig. 9 and 10). Slight induction of apoptosis was observed at lower concentration after treatment with compound **11k** after 48 h. Overall, the results showed that compound **11k** could induce cell apoptosis in a time- and dose-dependent manner.

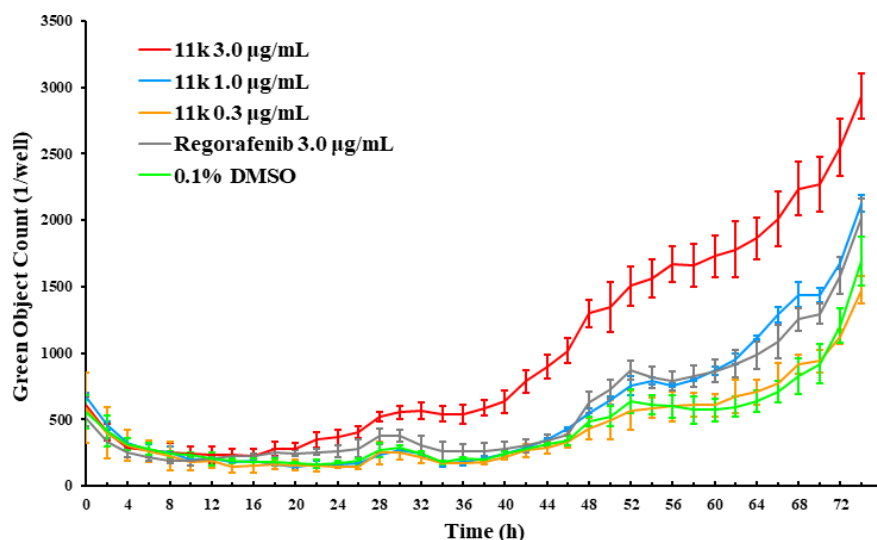


Fig. 9 The apoptosis curves of IncuCyte live-cell imaging assays in HT-29 cells. All error bars are expressed as mean \pm SD of three independent experiments. The cell population was monitored for 72 h using an IncuCyte ZOOM system in an incubator.

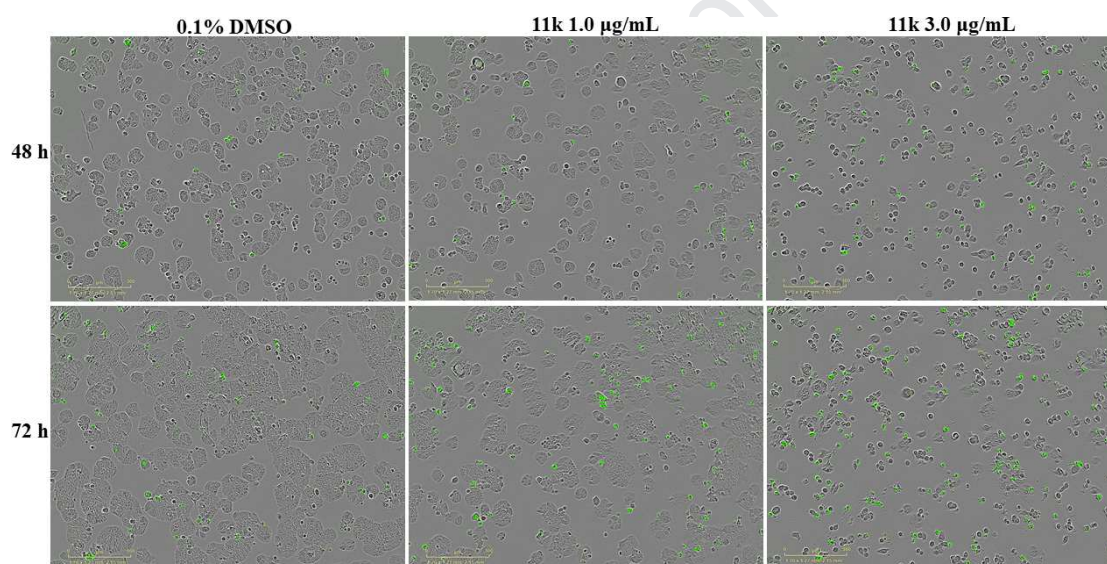


Fig. 10 The white light merged images of study on apoptosis on HT-29 cells after 48 h and 72 h of treatment with compound **11k** and 0.1% DMSO. Green fluorescent cells were counted as apoptotic cells. Nucleus were stained with the CellEvent[®] Caspase 3/7 Green ReadyProbes[®] reagent.

3.2.3.3. Antiproliferation and cytotoxicity against FHC

Inspired by the potent antitumor activity of compound **11k**, its kinetics of antiproliferation and cytotoxicity on human normal colorectal mucosa epithelial cell FHC was evaluated. As shown in Fig. 11A and Fig. 12, the confluence treated with 10.0 $\mu\text{g/mL}$ of compound **11k** reached to 26.7% after 72 h which was extremely weaker than that of Regorafenib (13.5%). Lower concentration could not efficiently inhibited cell proliferation (data not shown). A dose- and time-dependent increase of dead cell numbers was exhibited by treatment with compound **11k** (Fig. 11B and 12). The kinetics of cytotoxicity of compound **11k** (10.0 $\mu\text{g/mL}$) was almost equipotent to that of Regorafenib (0.19 $\mu\text{g/mL}$) during the treatment time. The above results indicated that compound **11k** was much less toxic to normal colorectal mucosa

epithelial cells than that of Regorafenib.

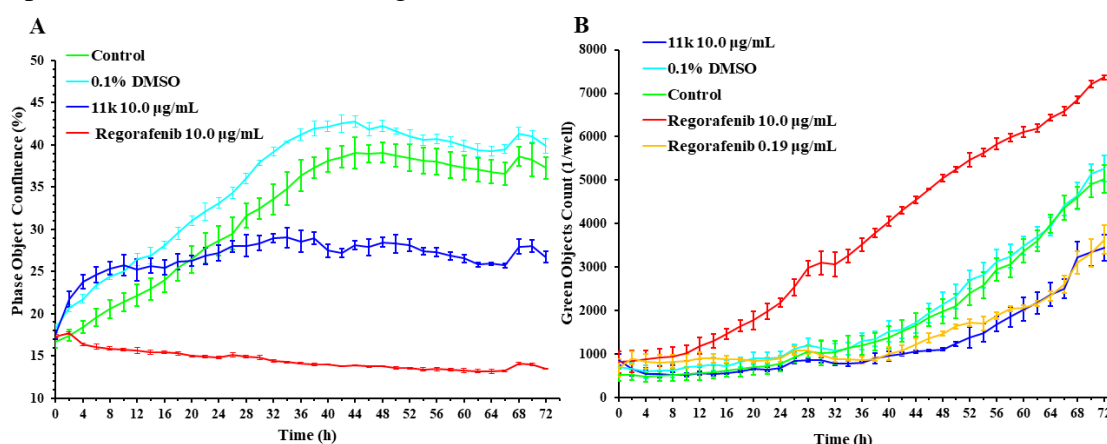


Fig. 11 The curves of InCuCyte live-cell imaging assays in FHC cell lines. All error bars are expressed as mean \pm SD of three independent experiments. A) The curves of real-time cell confluence. The cell population was monitored for 72 h using an InCuCyte ZOOM system in an incubator. B) The curves of real-time cytotoxicity. The dead cell population was monitored for 72 h using an InCuCyte ZOOM system in an incubator.

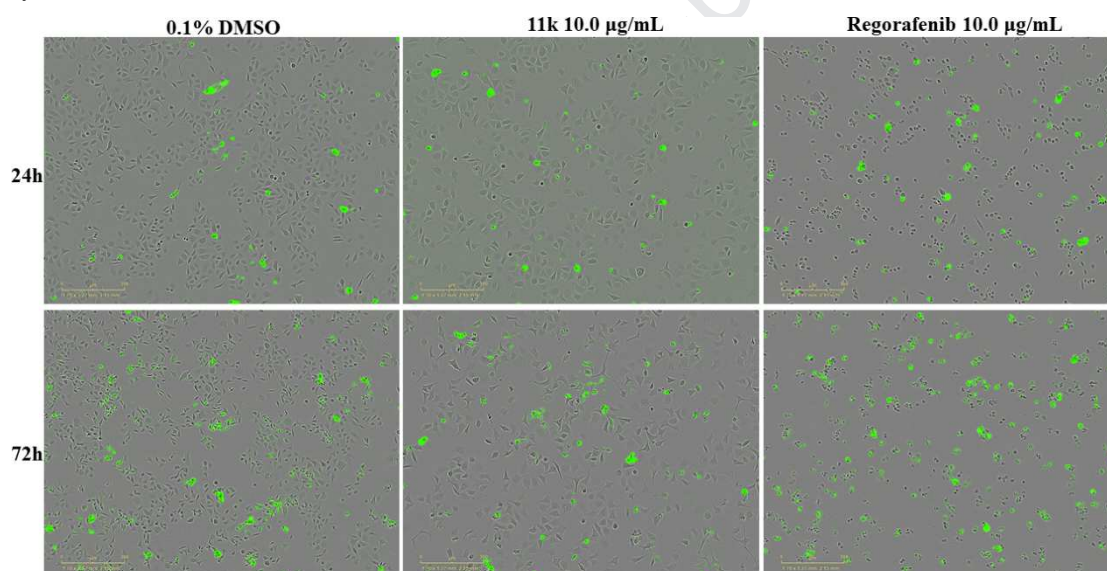


Fig. 12 The white light images (merged) of study on antiproliferation and cytotoxicity against FHC cells after 24 h and 72 h of treatment with compound **11k**, Regorafenib or 0.1% DMSO. Green fluorescent cells were counted as dead cell. Nucleus were stained with the DNA fluorescent probe YOYO-1 iodide.

3.2.4. Cell cycle analyses

Cell cycle analyses in HT-29 cells treated with compound **11k** and Regorafenib was performed. As shown in Fig. 13, no significant cell cycle arrest was found. Compound **11k** slightly induced cell cycle arrest with a G2/M percentage of 4.4% at 3.0 µg/mL compared to Regorafenib (2.0%) and 0.1% DMSO (2.4%). According to the results of weak cell cycle arrest and strong induction of apoptosis of compound **11k**, we could deduce that other factors inducing of apoptosis might be the targets of compound **11k**, such as p53, JNK, Bcl-2 and Caspases, *etc* [36-38].

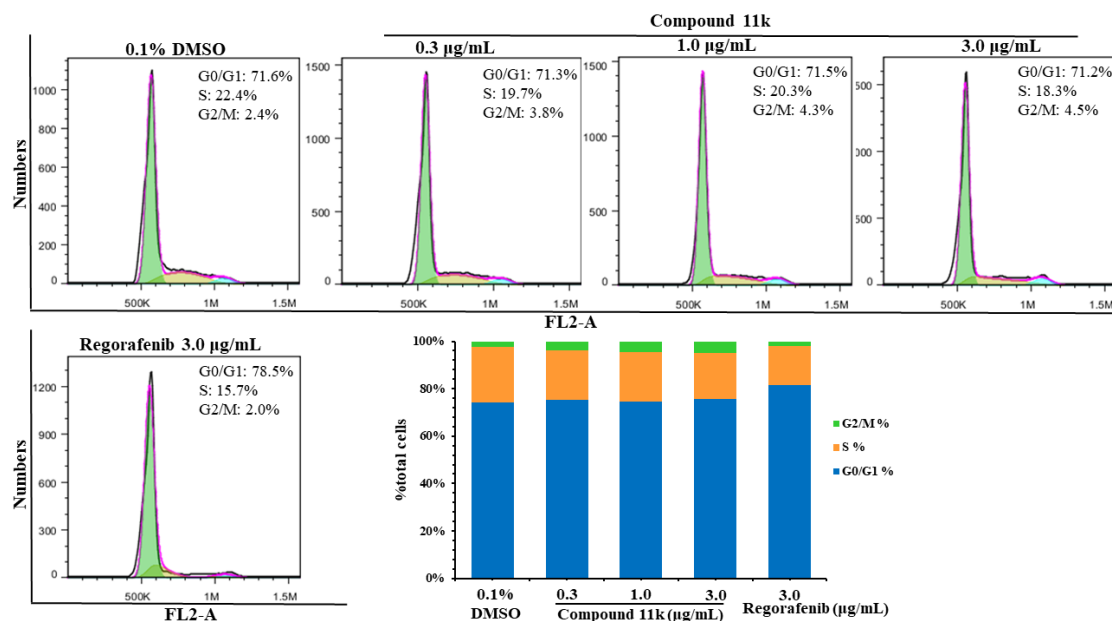


Fig. 13 Cell cycle progression analyses of HT-29 cells treated with compound **11k** and Regorafenib for 48 h.

3.2.5. *In vitro* kinase profile

In order to investigate the potential targets preliminarily, the most potent compound **11k** was screened against other six kinases, including c-Kit, B-Raf, c-Src, IGF1R, PDGFR α and AXL. As shown in Table 3, compound **11k** exhibited moderate inhibitory activity against several kinases, such as c-Met, Ron and PDGFR α , *etc.* The results indicated that compound **11k** was not a highly selective c-Met/Ron dual inhibitors. Thus, we deduced that the excellent anticancer activity might result from multiple kinases inhibitory activity, and other targets will be investigated in our future work.

Table 3 The kinase profile of compound **11k**.

Kinase	IC ₅₀ (μ M) ^a	Kinase	IC ₅₀ (μ M)
c-Met	0.382	PDGFR α	0.384
Ron	0.122	c-Src	0.421
c-Kit	>10.0	IGF1R	>10.0
AXL	0.632	B-Raf	>10.0

^a Values are expressed as the mean of two independent experiments.

4. Conclusions

In summary, a novel series of quinoline analogues bearing thiazolidinones were designed, synthesized and evaluated for their biological activities in the present work. Structure activity relationship analysis was performed based on biological evaluation and docking study, and the most potent 4-((4-(4-(3-(2-(2,6-difluorophenyl)-4-oxothiazolidin-3-yl)ureido)phenoxy)-6-methoxyquinolin-7-yl)oxy)-*N*-isopropylpiperidine-1-carboxamide (**11k**) was identified as a multi-kinase inhibitor. IncuCyte live-cell imaging assays indicated that compound **11k** performed excellent cytotoxicity, antiproliferation and induction of apoptosis on HT-29 cells in a time- and dose-dependent manner with an efficacy that was

significantly greater than Regorafenib. In addition, compound **11k** induced slight cell cycle arrest in the G2/M stage in HT-29 cells. The results of induction of apoptosis and cell cycle analysis indicated that other factors inducing of apoptosis might be the targets of compound **11k**. Further cell selectivity of compound **11k** showed that it was not active against human normal colorectal mucosa epithelial cell FHC at 10.0 $\mu\text{g/mL}$ or lower concentrations. The results of cell selectivity indicated that the toxicity to normal cells of compound **11k** was much lower than that of Regorafenib. The above results support further structural modification of compound **11k** to improve its inhibitory activity, which will lead to more potent kinase inhibitors as anticancer agents.

5. Experimental

5.1. Chemistry

Unless otherwise noted, all materials were obtained from commercial suppliers and used without further purification. ^1H NMR and ^{13}C NMR spectra were generated on Bruker ARX-400 spectrometers (Bruker Bioscience, Billerica, MA, USA). Chemical shifts are given in parts per million (ppm) relative to TMS as internal standards. Column chromatography was carried out on silica gel (200-300 mesh). High Resolution Mass spectra (HRMS) were taken in ESI mode on Agilent 6530 Q-TOF (Agilent Technologies, CA, USA).

5.1.1. General procedure for the synthesis of 2a-b. To a mixture of 7-(benzyloxy)-4-chloro-6-methoxyquinoline (50 g, 167.2 mmol) in dry PhCl (300 mL) was added 4-nitrophenol (418.1 mmol) for **2a** or 4-nitrothiophenol for **2b** (418.1 mmol). After refluxed for 16 h, the solvent was concentrated in vacuo, treated with CH_2Cl_2 (500 mL), and washed with 10% NaOH aqueous solution (3×100 mL) and water (100 mL). The organic layers were dried over MgSO_4 and concentrated give the crude products which were used for the next step without further purification.

5.1.1.1. 7-(benzyloxy)-6-methoxy-4-(4-nitrophenoxy)quinoline (2a). Tawny solid, yield: 62.4%. HRMS (ESI) m/z 403.1345 $[\text{M}+\text{H}]^+$, Calcd. for 403.1294.

5.1.1.2. 7-(benzyloxy)-6-methoxy-4-((4-nitrophenyl)thio)quinoline (2b). Brown solid, yield: 60.1%. HRMS (ESI) m/z 419.1102 $[\text{M}+\text{H}]^+$, Calcd. for 419.1066.

5.1.2. General procedure for the synthesis of 3a-b. Intermediates **2** (30.0 g) was slowly added to 33% HBr in HOAc (150 mL) and the mixtures were stirred for 3 h at room temperature during which time target products were precipitated. The mixture was filtrated, and the solid was washed with isopropyl ether to give the products.

5.1.2.1. 6-methoxy-4-(4-nitrophenoxy)quinolin-7-ol (3a). Light solid, yield: 66.4%. HRMS (ESI) m/z 313.0872 $[\text{M}+\text{H}]^+$, Calcd. for 313.0824.

5.1.2.2. 6-methoxy-4-((4-nitrophenyl)thio)quinolin-7-ol (3b). Beige solid, yield: 64.2%. HRMS (ESI) m/z 329.0653 $[\text{M}+\text{H}]^+$, Calcd. for 329.0596.

5.1.3. General procedure for the synthesis of 4a-c. To a mixture of intermediates **3a-b** (0.1 mol) in DMF (100 mL) was added caesium carbonate (0.25 mol) and the mixture was stirred vigorously at room temperature for 10 min. Different piperidines (0.15 mol) were added and the mixture was heated to 110 $^\circ\text{C}$ for 6 h. The reaction mixture was cooled to room temperature and poured into water (500 mL), filtered, and washed with water to give crude **4a-c** which were purified by silica gel column

chromatography (eluent, CH₂Cl₂:MeOH = 100:1 to 15:1) to afford **4a-c**.

5.1.3.1. *tert-butyl*
4-((6-methoxy-4-(4-nitrophenoxy)quinolin-7-yl)oxy)piperidine-1-carboxylate (**4a**).
Yellow solid, yield: 52.1%. HRMS (ESI) m/z 496.2166 [M+H]⁺, Calcd. for 496.2084.

5.1.3.2. *tert-butyl*
4-((6-methoxy-4-((4-nitrophenyl)thio)quinolin-7-yl)oxy)piperidine-1-carboxylate (**4b**).
Yellow solid, yield: 46.7%. HRMS (ESI) m/z 512.1913 [M+H]⁺, Calcd. for 512.1855.

5.1.3.3. *tert-butyl*
4-(((6-methoxy-4-(4-nitrophenoxy)quinolin-7-yl)oxy)methyl)piperidine-1-carboxylate
(**4c**). Yellow solid, yield: 55.3%. HRMS (ESI) m/z 510.2302 [M+H]⁺, Calcd. for
510.2240.

5.1.4. *General procedure for the synthesis of 5a-c*. To a mixture of intermediates **4** (50.0 mmol) and CH₂Cl₂ (100 mL) was added CF₃COOH (50 mL). The solution was stirred for 2 h at room temperature and concentrated in vacuo. CH₂Cl₂ (200 mL) was added to the residue and saturated NaHCO₃ aqueous solution was added until the pH was adjusted to 8. The organics were dried over Na₂SO₄, concentrated in vacuo, and the residue was used for the next step without further purification.

5.1.4.1. 6-methoxy-4-(4-nitrophenoxy)-7-(piperidin-4-yloxy)quinoline (**5a**). Dark yellow oil, yield: 79.6%. HRMS (ESI) m/z 396.1601 [M+H]⁺, Calcd. for 396.1559.

5.1.4.2. 6-methoxy-4-((4-nitrophenyl)thio)-7-(piperidin-4-yloxy)quinoline (**5b**). Dark yellow oil, yield: 74.8%. HRMS (ESI) m/z 412.1403 [M+H]⁺, Calcd. for 412.1331.

5.1.4.3. 6-methoxy-4-(4-nitrophenoxy)-7-(piperidin-4-ylmethoxy)quinoline (**5c**). Dark yellow oil, yield: 77.5%. HRMS (ESI) m/z 410.1764 [M+H]⁺, Calcd. for 410.1716.

5.1.5. *General procedure for the synthesis of 6a-g*. A solution of isocyanates (24.0 mmol) in dry CH₂Cl₂ (10 mL) was added dropwise to a cooled solution of intermediates **5a-c** (20.0 mmol) and Et₃N (30.0 mmol) in dry CH₂Cl₂ (100 mL). The mixture was then stirred for 3-5 h at room temperature. After complete conversion of the starting material, saturated NaHCO₃ aqueous solution (20 mL) was added. The organic phase was separated, dried over Na₂SO₄ overnight, and concentrated in vacuo to afford **6a-g**.

5.1.5.1.
N-ethyl-4-((6-methoxy-4-(4-nitrophenoxy)quinolin-7-yl)oxy)piperidine-1-carboxamide (**6a**). Yellow solid, yield: 82.9%. ¹H NMR (400 MHz, DMSO-*d*₆) δ: 8.44 (d, *J* = 5.2 Hz, 1H), 7.92 (m, 2H), 7.49 (s, 1H), 7.15 (m, 3H), 6.43 (d, *J* = 5.2 Hz, 1H), 3.92 (s, 3H), 3.64-3.70 (m, 1H), 3.09-3.16 (m, 4H), 2.95-3.02 (m, 2H), 1.98-2.02 (m, 2H), 1.67-1.73 (m, 2H), 1.02 (t, *J* = 7.2 Hz, 3H); HRMS (ESI) m/z 467.1983 [M+H]⁺, Calcd. for 467.1931.

5.1.5.2.
N-isopropyl-4-((6-methoxy-4-(4-nitrophenoxy)quinolin-7-yl)oxy)piperidine-1-carboxamide (**6b**). Yellow solid, yield: 84.2%. ¹H NMR (400 MHz, DMSO-*d*₆) δ: 8.46 (d, *J* = 5.2 Hz, 1H), 7.91 (m, 2H), 7.48 (s, 1H), 7.15 (m, 3H), 6.45 (d, *J* = 5.2 Hz, 1H), 3.93 (s, 3H), 3.66-3.72 (m, 1H), 3.10-3.16 (m, 3H), 2.95-3.02 (m, 2H), 1.98-2.01 (m, 2H),

1.52-1.61 (m, 2H), 1.07 (s, 3H), 1.06 (s, 3H); HRMS (ESI) m/z 481.2161 [M+H]⁺, Calcd. for 481.2087.

5.1.5.3.

N-butyl-4-((6-methoxy-4-(4-nitrophenoxy)quinolin-7-yl)oxy)piperidine-1-carboxamide (**6c**). Yellow solid, yield: 78.8%. HRMS (ESI) m/z 495.2268 [M+H]⁺, Calcd. for 495.2244.

5.1.5.4.

N-cyclohexyl-4-((6-methoxy-4-(4-nitrophenoxy)quinolin-7-yl)oxy)piperidine-1-carboxamide (**6d**). Yellow solid, yield: 76.4%. HRMS (ESI) m/z 537.2220 [M+H]⁺, Calcd. for 537.2172.

5.1.5.5.

N-benzyl-4-((6-methoxy-4-(4-nitrophenoxy)quinolin-7-yl)oxy)piperidine-1-carboxamide (**6e**). Light yellow solid, yield: 83.1%. HRMS (ESI) m/z 545.1908 [M+H]⁺, Calcd. for 545.1859.

5.1.5.6.

N-isopropyl-4-((6-methoxy-4-((4-nitrophenyl)thio)quinolin-7-yl)oxy)piperidine-1-carboxamide (**6f**). Yellow solid, yield: 78.7%. HRMS (ESI) m/z 497.1907 [M+H]⁺, Calcd. for 497.1859.

5.1.5.7.

N-isopropyl-4-(((6-methoxy-4-(4-nitrophenoxy)quinolin-7-yl)oxy)methyl)piperidine-1-carboxamide (**6g**). Yellow solid, yield: 78.2%. HRMS (ESI) m/z 511.2069 [M+H]⁺, Calcd. for 511.2015.

5.1.6. General procedure for the synthesis of **7a-g**. Powered iron (0.06 mol) and concentrated HCl (2 drops) was added to a suspension of intermediates **6a-g** (0.02 mol) in 90% EtOH (100 mL). The mixture was refluxed with vigorous agitation for 4-6 h. The hot mixture was filtered through celites and the filtrate was evaporated in vacuo to afford **7a-g**.

5.1.6.1.

4-((4-(4-aminophenoxy)-6-methoxyquinolin-7-yl)oxy)-*N*-ethylpiperidine-1-carboxamide (**7a**). Yellow solid, yield: 83.4%. HRMS (ESI) m/z 437.2243 [M+H]⁺, Calcd. for 437.2189.

5.1.6.2.

4-((4-(4-aminophenoxy)-6-methoxyquinolin-7-yl)oxy)-*N*-isopropylpiperidine-1-carboxamide (**7b**). Yellow solid, yield: 81.0%. HRMS (ESI) m/z 451.2397 [M+H]⁺, Calcd. for 451.2345.

5.1.6.3.

4-((4-(4-aminophenoxy)-6-methoxyquinolin-7-yl)oxy)-*N*-butylpiperidine-1-carboxamide (**7c**). Yellow solid, yield: 85.8%. HRMS (ESI) m/z 465.2574 [M+H]⁺, Calcd. for 465.2502.

5.1.6.4.

N-cyclohexyl-4-((6-methoxy-4-(4-nitrophenoxy)quinolin-7-yl)oxy)piperidine-1-carboxamide (**7d**). Yellow solid, yield: 78.9%. HRMS (ESI) m/z 491.2708 [M+H]⁺, Calcd. for 491.2658.

5.1.6.5.

4-((4-((4-aminophenyl)thio)-6-methoxyquinolin-7-yl)oxy)-*N*-benzylpiperidine-1-carboxamide (**7e**). Yellow solid, yield: 81.7%. HRMS (ESI) m/z 499.2407 $[M+H]^+$, Calcd. for 499.2345.

5.1.6.6.

4-((4-((4-aminophenyl)thio)-6-methoxyquinolin-7-yl)oxy)-*N*-isopropylpiperidine-1-carboxamide (**7f**). Yellow solid, yield: 80.4%. HRMS (ESI) m/z 467.2163 $[M+H]^+$, Calcd. for 467.2117.

5.1.6.7.

4-(((4-(4-aminophenoxy)-6-methoxyquinolin-7-yl)oxy)methyl)-*N*-isopropylpiperidine-1-carboxamide (**7g**). Yellow solid, yield: 77.4%. HRMS (ESI) m/z 481.2338 $[M+H]^+$, Calcd. for 481.2273.

5.1.7. General procedure for the synthesis of **9a-g**. To a solution of **7** (10.0 mmol) and dry pyridine (42.0 mmol) in dry CH_2Cl_2 (50 mL), phenyl chloroformate (20.0 mmol) in dry CH_2Cl_2 (5 mL) was added dropwise at 0 °C. After the addition was completed, the solution was stirred at room temperature for 2 h. Saturated $NaHCO_3$ aqueous solution (2×20 mL) was added to the above solution and the organic phase was separated, washed with 20 mL water, dried over anhydrous Na_2SO_4 , concentrated in vacuo to afford intermediates **8a-g**, which were immediately used in the following reaction without further purification.

80% Hydrazine monohydrate (15 mL) was added to a solution of **8a-g** in xylene (15 mL), and the mixture was stirred vigorously at 70 °C for 2 h. After cooling to room temperature, the solvent was concentrated under reduced pressure. The residue was purified by silica gel column chromatography (eluent, CH_2Cl_2 : MeOH: Et_3N = 100:2:1 to 100:10:1) to afford **9a-g**.

5.1.7.1.

N-ethyl-4-((4-(4-(hydrazinecarboxamido)phenoxy)-6-methoxyquinolin-7-yl)oxy)piperidine-1-carboxamide (**9a**). Light yellow solid, yield: 36.4% (two steps). HRMS (ESI) m/z 495.2414 $[M+H]^+$, Calcd. for 495.2356.

5.1.7.2.

4-((4-(4-(hydrazinecarboxamido)phenoxy)-6-methoxyquinolin-7-yl)oxy)-*N*-isopropylpiperidine-1-carboxamide (**9b**). Light yellow solid, yield: 39.8% (two steps). HRMS (ESI) m/z 509.2584 $[M+H]^+$, Calcd. for 509.2512.

5.1.7.3.

N-butyl-4-((4-(4-(hydrazinecarboxamido)phenoxy)-6-methoxyquinolin-7-yl)oxy)piperidine-1-carboxamide (**9c**). Light yellow solid, yield: 35.3% (two steps). HRMS (ESI) m/z 563.2734 $[M+H]^+$, Calcd. for 563.2669.

5.1.7.4.

N-cyclohexyl-4-((4-(4-(hydrazinecarboxamido)phenoxy)-6-methoxyquinolin-7-yl)oxy)piperidine-1-carboxamide (**9d**). Light yellow solid, yield: 41.5% (two steps). HRMS (ESI) m/z 549.2883 $[M+H]^+$, Calcd. for 549.2825.

5.1.7.5.

N-benzyl-4-((4-(4-(hydrazinecarboxamido)phenoxy)-6-methoxyquinolin-7-yl)oxy)piperidine-1-carboxamide (**9e**). Light yellow solid, yield: 31.9% (two steps). HRMS (ESI) m/z 557.2590 $[M+H]^+$, Calcd. for 557.2512.

5.1.7.6.

4-(((4-((4-(hydrazinecarboxamido)phenyl)thio)-6-methoxyquinolin-7-yl)oxy)-N-isopropylpiperidine-1-carboxamide (**9f**)). Light yellow solid, yield: 34.7% (two steps). HRMS (ESI) m/z 525.2352 [M+H]⁺, Calcd. for 525.2284.

5.1.7.7.

4-(((4-((4-(hydrazinecarboxamido)phenoxy)-6-methoxyquinolin-7-yl)oxy)methyl)-N-isopropylpiperidine-1-carboxamide (**9g**)). Light yellow solid, yield: 34.7% (two steps). HRMS (ESI) m/z 523.2761 [M+H]⁺, Calcd. for 523.2669.

5.1.8. *General procedure for the synthesis of 10a-o.* To a solution of semicarbazide **9a-g** (2.0 mmol) and aldehyde (2.4 mmol) in dry *i*-PrOH (10 mL), HOAc (2 drops) were added. After refluxing for 2 h, the mixture was cooled to 0 °C, and the resultant precipitate was filtered, washed with cold *i*-PrOH and dried under vacuum to afford **10a-o**. If no precipitate appeared, silica gel column chromatography (eluent, CH₂Cl₂: MeOH: Et₃N = 100:2:1 to 100:10:1) was used to isolate the target compounds.

5.1.8.1.

(*E*)-*N*-ethyl-4-(((4-((2-(4-fluorobenzylidene)hydrazine-1-carboxamido)phenoxy)-6-methoxyquinolin-7-yl)oxy)piperidine-1-carboxamide (**10a**)). White solid, yield: 85.0%. HRMS (ESI) m/z 601.2617 [M+H]⁺, Calcd. for 601.2575.

5.1.8.2.

(*E*)-4-(((4-((2-(4-fluorobenzylidene)hydrazine-1-carboxamido)phenoxy)-6-methoxyquinolin-7-yl)oxy)-N-isopropylpiperidine-1-carboxamide (**10b**)). White solid, yield: 81.6%. HRMS (ESI) m/z 615.2783 [M+H]⁺, Calcd. for 615.2731.

5.1.8.3.

(*E*)-*N*-butyl-4-(((4-((2-(4-fluorobenzylidene)hydrazine-1-carboxamido)phenoxy)-6-methoxyquinolin-7-yl)oxy)piperidine-1-carboxamide (**10c**)). White solid, yield: 83.1%. HRMS (ESI) m/z 629.2937 [M+H]⁺, Calcd. for 629.2888.

5.1.8.4.

(*E*)-*N*-cyclohexyl-4-(((4-((2-(4-fluorobenzylidene)hydrazine-1-carboxamido)phenoxy)-6-methoxyquinolin-7-yl)oxy)piperidine-1-carboxamide (**10d**)). White solid, yield: 82.4%. HRMS (ESI) m/z 655.3102 [M+H]⁺, Calcd. for 655.3044.

5.1.8.5.

(*E*)-*N*-benzyl-4-(((4-((2-(4-fluorobenzylidene)hydrazine-1-carboxamido)phenoxy)-6-methoxyquinolin-7-yl)oxy)piperidine-1-carboxamide (**10e**)). White solid, yield: 86.1%. HRMS (ESI) m/z 663.2783 [M+H]⁺, Calcd. for 663.2731.

5.1.8.6.

(*E*)-4-(((4-((2-benzylidenehydrazine-1-carboxamido)phenoxy)-6-methoxyquinolin-7-yl)oxy)-N-isopropylpiperidine-1-carboxamide (**10f**)). White solid, yield: 78.7%. HRMS (ESI) m/z 597.2877 [M+H]⁺, Calcd. for 597.2825.

5.1.8.7.

(*E*)-4-(((4-((2-(3,4-difluorobenzylidene)hydrazine-1-carboxamido)phenoxy)-6-methoxyquinolin-7-yl)oxy)-N-isopropylpiperidine-1-carboxamide (**10g**)). White solid, yield: 84.7%. HRMS (ESI) m/z 633.2701 [M+H]⁺, Calcd. for 633.2637.

5.1.8.8.

(*E*)-4-(((4-((2-(2,3-difluorobenzylidene)hydrazine-1-carboxamido)phenoxy)-6-methoxyquinolin-7-yl)oxy)-N-isopropylpiperidine-1-carboxamide (**10h**)). White solid, yield: 84.7%. HRMS (ESI) m/z 633.2701 [M+H]⁺, Calcd. for 633.2637.

xyquinolin-7-yl)oxy)-N-isopropylpiperidine-1-carboxamide (10h). White solid, yield: 83.9%. HRMS (ESI) m/z 633.2703 $[M+H]^+$, Calcd. for 633.2637.

5.1.8.9.

(E)-4-((4-(4-(2-(2-fluorobenzylidene)hydrazine-1-carboxamido)phenoxy)-6-methoxyquinolin-7-yl)oxy)-N-isopropylpiperidine-1-carboxamide (10i). White solid, yield: 82.6%. HRMS (ESI) m/z 615.2803 $[M+H]^+$, Calcd. for 615.2731.

5.1.8.10.

(E)-4-((4-(4-(2-(2,4-difluorobenzylidene)hydrazine-1-carboxamido)phenoxy)-6-methoxyquinolin-7-yl)oxy)-N-isopropylpiperidine-1-carboxamide (10j). White solid, yield: 82.0%. HRMS (ESI) m/z 633.2701 $[M+H]^+$, Calcd. for 633.2637.

5.1.8.11.

(E)-4-((4-(4-(2-(2,6-difluorobenzylidene)hydrazine-1-carboxamido)phenoxy)-6-methoxyquinolin-7-yl)oxy)-N-isopropylpiperidine-1-carboxamide (10k). White solid, yield: 80.1%. HRMS (ESI) m/z 633.2705 $[M+H]^+$, Calcd. for 633.2637.

5.1.8.12.

(E)-4-((4-(4-(2-(3-fluorobenzylidene)hydrazine-1-carboxamido)phenoxy)-6-methoxyquinolin-7-yl)oxy)-N-isopropylpiperidine-1-carboxamide (10l). White solid, yield: 76.9%. HRMS (ESI) m/z 615.2801 $[M+H]^+$, Calcd. for 615.2731.

5.1.8.13.

(E)-N-isopropyl-4-((6-methoxy-4-(4-(2-(2,4,6-trifluorobenzylidene)hydrazine-1-carboxamido)phenoxy)quinolin-7-yl)oxy)piperidine-1-carboxamide (10m). White solid, yield: 80.7%. HRMS (ESI) m/z 651.2605 $[M+H]^+$, Calcd. for 651.2543.

5.1.8.14.

(E)-4-((4-(4-(2-(2,6-difluorobenzylidene)hydrazine-1-carboxamido)phenylthio)-6-methoxyquinolin-7-yl)oxy)-N-isopropylpiperidine-1-carboxamide (10n). White solid, yield: 77.7%. HRMS (ESI) m/z 649.2473 $[M+H]^+$, Calcd. for 649.2409.

5.1.8.15.

(E)-4-(((4-(4-(2-(2,6-difluorobenzylidene)hydrazine-1-carboxamido)phenoxy)-6-methoxyquinolin-7-yl)oxy)methyl)-N-isopropylpiperidine-1-carboxamide (10o). White solid, yield: 83.5%. HRMS (ESI) m/z 647.2855 $[M+H]^+$, Calcd. for 647.2793.

5.1.9. General procedure for the synthesis of target compounds 11a-o. To a solution of semicarbazides **10a-o** (0.5 mmol) and mercaptoacetic acid (0.5 mL) in dry CH_2Cl_2 (10 mL), SiCl_4 (20 drops) were added at room temperature. After the resulting mixture refluxed for 6 h, the reaction mixture was cooled to room temperature before quenched by ice. The solution was adjusted to pH 9 with 10% NaOH aqueous solution. The organic phase was separated and washed with water (2x5 mL), concentrated in vacuo to afford yellow oil which was purified by silica gel column chromatography (eluent, CH_2Cl_2 : MeOH: Et_3N = 100:5:1 to 100:10:1) to afford target compounds.

5.1.9.1.

N-ethyl-4-((4-(4-(3-(2-(4-fluorophenyl)-4-oxothiazolidin-3-yl)ureido)phenoxy)-6-methoxyquinolin-7-yl)oxy)piperidine-1-carboxamide (11a). White solid, yield: 36.3%. ^1H NMR (400 MHz, $\text{DMSO}-d_6$) δ : 9.45 (br, 1H), 9.06 (br, 1H), 8.45 (d, J = 5.2 Hz, 1H), 7.52-7.57 (m, 5H), 7.49 (s, 1H), 7.21-7.25 (m, 2H), 7.17 (m, 1H), 7.14 (m, 1H),

6.50-6.53 (m, 1H), 6.40 (d, $J = 5.2$ Hz, 1H), 5.85 (s, 1H), 4.76-4.82 (m, 1H), 3.93 (s, 3H), 3.85-3.89 (m, 1H), 3.72-3.77 (m, 3H), 3.09-3.17 (m, 2H), 3.20-3.07 (m, 2H), 1.98-2.02 (m, 2H), 1.53-1.60 (m, 2H), 1.02 (t, $J = 7.2$ Hz, 3H); ^{13}C NMR (100 MHz, DMSO- d_6) δ : 169.4, 161.7, 160.6, 157.4 (2C), 154.2, 150.5, 149.3, 149.0, 146.7, 137.2, 132.3, 131.9, 121.9 (2C), 116.0, 115.9, 115.7, 115.2, 112.9, 112.7, 110.8, 103.3, 100.1, 73.9, 56.9, 56.2, 42.0, 41.5 (2C), 30.7 (2C), 29.6, 13.9. HRMS (ESI) m/z 697.2304 $[\text{M}+\text{Na}]^+$, Calcd. for 697.2221.

5.1.9.2.

4-((4-(4-(3-(2-(4-fluorophenyl)-4-oxothiazolidin-3-yl)ureido)phenoxy)-6-methoxyquinolin-7-yl)oxy)-*N*-isopropylpiperidine-1-carboxamide (**11b**). White solid, yield: 41.7%. ^1H NMR (400 MHz, DMSO- d_6) δ : 8.97 (br, 1H), 8.54 (s, 1H), 8.45 (d, $J = 5.2$ Hz, 1H), 7.52-7.58 (m, 5H), 7.49 (s, 1H), 7.22-7.26 (m, 2H), 7.18 (m, 1H), 7.15 (m, 1H), 6.41 (d, $J = 5.2$ Hz, 1H), 6.22 (m, 1H), 5.85 (s, 1H), 4.77-4.81 (m, 1H), 3.93 (s, 3H), 3.86-3.90 (m, 1H), 3.73-3.81 (m, 4H), 3.09-3.16 (m, 2H), 1.98-2.01 (m, 2H), 1.52-1.61 (m, 2H), 1.07 (s, 3H), 1.06 (s, 3H); ^{13}C NMR (100 MHz, DMSO- d_6) δ : 169.7, 161.8, 160.6, 157.3 (2C), 154.2, 150.5, 149.3, 149.0, 146.7, 137.2, 132.1, 131.9, 121.9 (2C), 116.0, 115.9, 115.7, 115.2, 112.9, 112.7, 110.8, 103.3, 100.1, 73.9, 56.9, 56.2, 42.3, 41.5 (2C), 30.7 (2C), 29.6, 23.4 (2C). HRMS (ESI) m/z 711.2481 $[\text{M}+\text{Na}]^+$, Calcd. for 711.2377.

5.1.9.3.

N-butyl-4-((4-(4-(3-(2-(4-fluorophenyl)-4-oxothiazolidin-3-yl)ureido)phenoxy)-6-methoxyquinolin-7-yl)oxy)piperidine-1-carboxamide (**11c**). White solid, yield: 40.4%. ^1H NMR (400 MHz, DMSO- d_6) δ : 8.97 (br, 1H), 8.54 (s, 1H), 8.45 (d, $J = 5.2$ Hz, 1H), 7.51-7.58 (m, 5H), 7.49 (s, 1H), 7.22-7.26 (m, 2H), 7.18 (m, 1H), 7.15 (m, 1H), 6.49 (m, 1H), 6.41 (d, $J = 5.2$ Hz, 1H), 5.85 (s, 1H), 4.77-4.81 (m, 1H), 3.92 (s, 3H), 3.86-3.90 (m, 1H), 3.73-3.79 (m, 3H), 3.10-3.17 (m, 2H), 3.00-3.05 (m, 2H), 1.98-2.01 (m, 2H), 1.52-1.60 (m, 2H), 1.36-1.43 (m, 2H), 1.23-1.32 (m, 2H), 0.88 (m, 3H). HRMS (ESI) m/z 725.2625 $[\text{M}+\text{Na}]^+$, Calcd. for 725.2534.

5.1.9.4.

N-cyclohexyl-4-((4-(4-(3-(2-(4-fluorophenyl)-4-oxothiazolidin-3-yl)ureido)phenoxy)-6-methoxyquinolin-7-yl)oxy)piperidine-1-carboxamide (**11d**). White solid, yield: 40.0%. ^1H NMR (400 MHz, DMSO- d_6) δ : 8.94 (br, 1H), 8.51 (s, 1H), 8.45 (d, $J = 5.2$ Hz, 1H), 7.51-7.58 (m, 5H), 7.49 (s, 1H), 7.22-7.26 (m, 2H), 7.18 (m, 1H), 7.15 (m, 1H), 6.40 (d, $J = 5.2$ Hz, 1H), 6.21 (m, 1H), 5.84 (s, 1H), 4.76-4.80 (m, 1H), 3.92 (s, 3H), 3.86-3.91 (m, 1H), 3.72-3.79 (m, 3H), 3.09-3.16 (m, 2H), 1.97-2.01 (m, 2H), 1.74-1.77 (m, 2H), 1.67-1.70 (m, 2H), 1.52-1.59 (m, 3H), 1.18-1.28 (m, 4H), 1.05-1.15 (m, 2H); 1.07 (s, 3H), 1.06 (s, 3H). HRMS (ESI) m/z 751.2791 $[\text{M}+\text{Na}]^+$, Calcd. for 751.2690.

5.1.9.5.

N-benzyl-4-((4-(4-(3-(2-(4-fluorophenyl)-4-oxothiazolidin-3-yl)ureido)phenoxy)-6-methoxyquinolin-7-yl)oxy)piperidine-1-carboxamide (**11e**). Light yellow solid, yield: 41.3%, purity: 98.24%. ^1H NMR (400 MHz, DMSO- d_6) δ : 9.06 (br, 1H), 8.64 (br, 1H), 8.45 (d, $J = 5.2$ Hz, 1H), 7.52-7.58 (m, 5H), 7.50 (s, 1H), 7.30-7.33 (m, 2H), 7.19-7.27 (m, 6H), 7.13-7.18 (m, 3H), 6.41 (d, $J = 5.2$ Hz, 1H), 5.83 (s, 1H),

4.79-4.84 (m, 1H), 4.27 (m, 2H), 3.93 (s, 3H), 3.74-3.90 (m, 5H), 3.17-3.23 (m, 2H), 2.01-2.04 (m, 2H), 1.55-1.64 (m, 2H). HRMS (ESI) m/z 759.2481 $[M+Na]^+$, Calcd. for 759.2377.

5.1.9.6.

N-isopropyl-4-((6-methoxy-4-(4-(3-(4-oxo-2-phenylthiazolidin-3-yl)ureido)phenoxy)quinolin-7-yl)oxy)piperidine-1-carboxamide (II f). White solid, yield: 44.6%. 1H NMR (400 MHz, DMSO- d_6) δ : 8.95 (br, 1H), 8.55 (s, 1H), 8.45 (d, $J = 5.2$ Hz, 1H), 7.49-7.54 (m, 6H), 7.35-7.43 (m, 3H), 7.18 (m, 1H), 7.15 (m, 1H), 6.41 (d, $J = 5.2$ Hz, 1H), 6.22 (m, 1H), 5.83 (s, 1H), 4.76-4.82 (m, 1H), 3.93 (s, 3H), 3.83-3.89 (m, 1H), 3.73-3.79 (m, 4H), 3.10-3.16 (m, 2H), 1.97-2.01 (m, 2H), 1.52-1.61 (m, 2H), 1.07 (s, 3H), 1.06 (s, 3H); ^{13}C NMR (100 MHz, DMSO- d_6) δ : 169.7, 164.0, 160.5, 157.3 (2C), 154.2, 150.5, 149.3, 149.0, 146.8, 137.1, 132.2, 131.9, 121.9 (2C), 120.7, 115.7, 115.4, 115.2, 112.9, 112.7, 110.8, 103.4, 100.1, 73.8, 56.9, 56.2, 42.3, 41.5 (2C), 30.7 (2C), 29.6, 23.4 (2C). HRMS (ESI) m/z 693.2539 $[M+Na]^+$, Calcd. for 693.2471.

5.1.9.7.

4-((4-(4-(3-(2-(3,4-difluorophenyl)-4-oxothiazolidin-3-yl)ureido)phenoxy)-6-methoxyquinolin-7-yl)oxy)-N-isopropylpiperidine-1-carboxamide (II g). White solid, yield: 44.7%. 1H NMR (400 MHz, DMSO- d_6) δ : 9.01 (s, 1H), 8.57 (s, 1H), 8.45 (d, $J = 5.2$ Hz, 1H), 7.64-7.68 (m, 1H), 7.43-7.54 (m, 5H), 7.36-7.38 (m, 1H), 7.18 (m, 1H), 7.16 (m, 1H), 6.41 (d, $J = 5.2$ Hz, 1H), 6.22 (m, 1H), 5.85 (s, 1H), 4.77-4.82 (m, 1H), 3.93 (s, 3H), 3.90-3.94 (m, 1H), 3.74-3.81 (m, 4H), 3.10-3.16 (m, 2H), 1.97-2.01 (m, 2H), 1.52-1.61 (m, 2H), 1.07 (s, 3H), 1.06 (s, 3H). HRMS (ESI) m/z 729.2386 $[M+Na]^+$, Calcd. for 729.2283.

5.1.9.8.

4-((4-(4-(3-(2-(2,3-difluorophenyl)-4-oxothiazolidin-3-yl)ureido)phenoxy)-6-methoxyquinolin-7-yl)oxy)-N-isopropylpiperidine-1-carboxamide (II h). White solid, yield: 40.1%. 1H NMR (400 MHz, DMSO- d_6) δ : 9.02 (s, 1H), 8.72 (s, 1H), 8.45 (d, $J = 5.2$ Hz, 1H), 7.52-7.55 (m, 3H), 7.48 (s, 1H), 7.44-7.47 (m, 2H), 7.25-7.30 (m, 1H), 7.19 (m, 1H), 7.17 (m, 1H), 6.41 (d, $J = 5.2$ Hz, 1H), 6.22 (m, 1H), 6.07 (s, 1H), 4.77-4.81 (m, 1H), 3.93 (s, 3H), 3.73-3.89 (m, 5H), 3.10-3.16 (m, 2H), 1.97-2.02 (m, 2H), 1.52-1.61 (m, 2H), 1.08 (s, 3H), 1.06 (s, 3H); ^{13}C NMR (100 MHz, DMSO- d_6) δ : 169.2, 164.0, 160.5, 157.3 (2C), 154.2, 150.5, 149.3, 149.0, 146.8, 137.1, 132.2, 131.4, 121.9 (2C), 120.7, 115.7, 115.4, 115.0, 112.9, 112.8, 110.8, 103.4, 100.1, 73.8, 56.9, 56.2, 42.3, 41.5 (2C), 30.8 (2C), 29.6, 23.3 (2C). HRMS (ESI) m/z 729.2386 $[M+Na]^+$, Calcd. for 729.2283.

5.1.9.9.

4-((4-(4-(3-(2-(2-fluorophenyl)-4-oxothiazolidin-3-yl)ureido)phenoxy)-6-methoxyquinolin-7-yl)oxy)-N-isopropylpiperidine-1-carboxamide (II i). White solid, yield: 45.8%. 1H NMR (400 MHz, DMSO- d_6) δ : 8.99 (br, 1H), 8.61 (s, 1H), 8.45 (d, $J = 5.2$ Hz, 1H), 7.52-7.55 (m, 3H), 7.49 (s, 1H), 7.39-7.48 (m, 2H), 7.32-7.34 (m, 1H), 7.20-7.22 (m, 1H), 7.18 (m, 1H), 7.16 (m, 1H), 6.41 (d, $J = 5.2$ Hz, 1H), 6.22 (m, 1H), 5.86 (s, 1H), 4.76-4.81 (m, 1H), 3.93 (s, 3H), 3.89 (m, 1H), 3.74-3.79 (m, 4H), 3.09-3.16 (m, 2H), 1.97-2.01 (m, 2H), 1.53-1.61 (m, 2H), 1.07 (s, 3H), 1.06 (s, 3H). HRMS (ESI) m/z 711.2492 $[M+Na]^+$, Calcd. for 711.2377.

5.1.9.10.

4-((4-(4-(3-(2-(2,4-difluorophenyl)-4-oxothiazolidin-3-yl)ureido)phenoxy)-6-methoxyquinolin-7-yl)oxy)-*N*-isopropylpiperidine-1-carboxamide (**11j**). White solid, yield: 38.6%. ¹H NMR (400 MHz, DMSO-*d*₆) δ: 9.07 (br, 1H), 8.70 (s, 1H), 8.45 (d, *J* = 5.2 Hz, 1H), 7.68-7.74 (m, 1H), 7.52-7.55 (m, 3H), 7.49 (s, 1H), 7.29-7.33 (m, 1H), 7.16-7.19 (m, 3H), 6.41 (d, *J* = 5.2 Hz, 1H), 6.22 (m, 1H), 6.04 (s, 1H), 4.76-4.82 (m, 1H), 3.93 (s, 3H), 3.86-3.90 (m, 1H), 3.79-3.80 (m, 1H), 3.73-3.78 (m, 3H), 3.09-3.16 (m, 2H), 1.97-2.01 (m, 2H), 1.52-1.61 (m, 2H), 1.07 (s, 3H), 1.06 (s, 3H). HRMS (ESI) *m/z* 729.2411 [M+Na]⁺, Calcd. for 729.2283.

5.1.9.11.

4-((4-(4-(3-(2-(2,6-difluorophenyl)-4-oxothiazolidin-3-yl)ureido)phenoxy)-6-methoxyquinolin-7-yl)oxy)-*N*-isopropylpiperidine-1-carboxamide (**11k**). White solid, yield: 38.9%, purity: 99.65%. ¹H NMR (400 MHz, DMSO-*d*₆) δ: 9.04 (s, 1H, NH), 8.84 (s, 1H, NH), 8.45 (d, *J* = 5.2 Hz, 1H, quinoline-2H), 7.50-7.54 (m, 4H, Ar-H), 7.49 (s, 1H, Ar-H), 7.16-7.20 (m, 4H, Ar-H), 6.41 (d, *J* = 5.2 Hz, 1H, quinoline-3H), 6.22 (m, 1H, NH), 6.17 (s, 1H, thiazolidinone-2H), 4.76-4.82 (m, 1H, isopropyl-H), 3.93 (s, 3H, CH₃O-), 3.79-3.83 (s, 2H, thiazolidinone-5H), 3.73-3.80 (m, 3H, piperidiny-H), 3.10-3.16 (m, 2H, piperidiny-H), 1.97-2.01 (m, 2H, piperidiny-H), 1.52-1.61 (m, 2H, piperidiny-H), 1.07 (s, 3H, isopropyl-H), 1.06 (s, 3H, isopropyl-H); ¹³C NMR (100 MHz, DMSO-*d*₆) δ: 169.7, 164.0, 160.6, 157.3 (2C), 154.2, 150.5, 149.3, 149.0, 146.8, 137.1, 132.1, 131.9, 121.9 (2C), 120.7, 115.7, 115.4, 115.2, 112.9, 112.7, 110.8, 103.4, 100.1, 73.9, 56.9, 56.2, 42.3, 41.5 (2C), 30.7 (2C), 29.6, 23.4 (2C). HRMS (ESI) *m/z* 729.2411 [M+Na]⁺, Calcd. for 729.2283.

5.1.9.12.

4-((4-(4-(3-(2-(3-fluorophenyl)-4-oxothiazolidin-3-yl)ureido)phenoxy)-6-methoxyquinolin-7-yl)oxy)-*N*-isopropylpiperidine-1-carboxamide (**11l**). White solid, yield: 38.9%. ¹H NMR (400 MHz, DMSO-*d*₆) δ: 9.01 (s, 1H), 8.68 (s, 1H), 8.45 (d, *J* = 5.2 Hz, 1H), 7.61-7.65 (m, 1H), 7.52-7.54 (m, 3H), 7.49 (s, 1H), 7.41-7.46 (m, 1H), 7.23-7.29 (m, 2H), 7.18 (m, 1H), 7.16 (m, 1H), 6.41 (d, *J* = 5.2 Hz, 1H), 6.22 (m, 1H), 6.07 (s, 1H), 4.76-4.81 (m, 1H), 3.93 (s, 3H), 3.86-3.90 (m, 1H), 3.79-3.81 (m, 1H), 3.73-3.77 (m, 3H), 3.10-3.16 (m, 2H), 1.97-2.02 (m, 2H), 1.52-1.60 (m, 2H), 1.07 (s, 3H), 1.06 (s, 3H). HRMS (ESI) *m/z* 711.2452 [M+Na]⁺, Calcd. for 711.2377.

5.1.9.13.

N-isopropyl-4-((6-methoxy-4-(4-(3-(4-oxo-2-(2,4,6-trifluorophenyl)thiazolidin-3-yl)ureido)phenoxy)quinolin-7-yl)oxy)piperidine-1-carboxamide (**11m**). White solid, yield: 36.7%. ¹H NMR (400 MHz, DMSO-*d*₆) δ: 9.04 (s, 1H), 8.80 (s, 1H), 8.45 (d, *J* = 5.2 Hz, 1H), 7.52-7.54 (m, 3H), 7.49 (s, 1H), 7.28-7.32 (m, 2H), 7.19 (m, 1H), 7.17 (m, 1H), 6.42 (d, *J* = 5.2 Hz, 1H), 6.22 (m, 1H), 6.11 (s, 1H), 4.77-4.80 (m, 1H), 3.93 (s, 3H), 3.82-3.87 (m, 2H), 3.74-3.79 (m, 3H), 3.10-3.15 (m, 2H), 1.97-2.01 (m, 2H), 1.53-1.60 (m, 2H), 1.08 (s, 3H), 1.06 (s, 3H). HRMS (ESI) *m/z* 747.2342 [M+Na]⁺, Calcd. for 747.2189.

5.1.9.14.

4-((4-((4-(3-(2-(2,6-difluorophenyl)-4-oxothiazolidin-3-yl)ureido)phenylthio)-6-methoxyquinolin-7-yl)oxy)-*N*-isopropylpiperidine-1-carboxamide (**11n**). White solid, yield:

39.5%. ¹H NMR (400 MHz, DMSO-*d*₆) δ: 9.14 (s, 1H), 8.86 (s, 1H), 8.40 (d, *J* = 5.2 Hz, 1H), 7.58-7.60 (m, 2H), 7.47-7.53 (m, 4H), 7.32 (s, 1H), 7.16-7.20 (m, 2H), 6.61 (d, *J* = 5.2 Hz, 1H), 6.22 (m, 1H), 6.16 (s, 1H), 4.76-4.82 (m, 1H), 3.93 (s, 3H), 3.84 (s, 2H), 3.73-3.79 (m, 3H), 3.08-3.15 (m, 2H), 1.97-2.01 (m, 2H), 1.51-1.60 (m, 2H), 1.07 (s, 3H), 1.06 (s, 3H); ¹³C NMR (100 MHz, DMSO-*d*₆) δ: 169.7, 163.7, 160.5, 157.3 (2C), 150.5, 149.3, 149.0, 146.8, 137.1, 132.2, 131.9, 130.5, 121.9 (2C), 120.7, 115.7, 115.4, 115.2, 112.9, 112.7, 110.8, 103.4, 100.2, 73.8, 56.9, 56.2, 42.4, 41.5 (2C), 30.6 (2C), 29.6, 23.4 (2C). HRMS (ESI) *m/z* 745.2191 [M+Na]⁺, Calcd. for 745.2054.

5.1.9.15.

4-(((4-(4-(3-(2-(2,6-difluorophenyl)-4-oxothiazolidin-3-yl)ureido)phenoxy)-6-methoxyquinolin-7-yl)oxy)methyl)-*N*-isopropylpiperidine-1-carboxamide (**11o**). White solid, yield: 40.8%, purity: 97.35%. ¹H NMR (400 MHz, DMSO-*d*₆) δ: 9.02 (s, 1H), 8.81 (s, 1H), 8.45 (d, *J* = 5.2 Hz, 1H), 7.48-7.54 (m, 4H), 7.38 (s, 1H), 7.16-7.20 (m, 4H), 6.42 (d, *J* = 5.2 Hz, 1H), 6.17 (s, 1H), 6.09-6.11 (m, 1H), 4.76-4.82 (m, 1H), 4.00-4.03 (m, 4H), 3.93 (s, 3H), 3.83 (s, 2H), 3.73-3.77 (m, 1H), 2.64-2.70 (m, 2H), 2.01 (br, 1H), 1.76-1.78 (m, 2H), 1.16-1.25 (m, 2H), 1.06 (s, 3H), 1.05 (s, 3H). HRMS (ESI) *m/z* 743.2507 [M+Na]⁺, Calcd. for 743.2439.

5.1.10.

3-(((4-(4-(3-(2-(2,6-difluorophenyl)-4-oxothiazolidin-3-yl)ureido)phenoxy)-6-methoxyquinolin-7-yl)oxy)-*N*-isopropylpiperidine-1-carboxamide (**19**). Taking intermediate **3a** and tert-butyl 3-((methylsulfonyl)oxy)piperidine-1-carboxylate as starting materials, target compound was prepared following the synthetic procedure of **11k**. White solid, yield: 34.8%. ¹H NMR (400 MHz, DMSO-*d*₆) δ: 9.03 (s, 1H), 8.84 (s, 1H), 8.44 (d, *J* = 5.2 Hz, 1H), 7.49-7.54 (m, 4H), 7.47 (s, 1H), 7.16-7.21 (m, 4H), 6.42 (d, *J* = 5.2 Hz, 1H), 6.21 (m, 1H), 6.16 (s, 1H), 4.76-4.81 (m, 1H), 3.92 (s, 3H), 3.79-3.83 (m, 2H), 3.73-3.79 (m, 3H), 3.10-3.17 (m, 2H), 1.89-1.96 (m, 2H), 1.48-1.59 (m, 2H), 1.07 (s, 3H), 1.06 (s, 3H). HRMS (ESI) *m/z* 729.2411 [M+Na]⁺, Calcd. for 729.2283.

5.1.11. 7-(benzyloxy)-6-methoxy-4-(4-nitrophenoxy)quinoline 1-oxide (**20**). Intermediate **2a** (20.1 g, 50.0 mmol) in CH₂Cl₂ (200 mL) was treated with *m*-CPBA (10.4 g, 60.0 mmol) at room temperature for 6 h. The reaction mixture was washed with NaHCO₃ aqueous solution (30 mL) and water (30 mL). The organic phase was separated, dried over Na₂SO₄, and evaporated under vacuum to afford **20** as yellow solid, yield: 67.7%. HRMS (ESI) *m/z* 419.1309 [M+H]⁺, Calcd. for 419.1243.

5.1.12.

7-(((1-(isopropylcarbamoyl)piperidin-4-yl)oxy)-6-methoxy-4-(4-nitrophenoxy)quinoline 1-oxide (**24**). Prepared by the method described for the synthesis of intermediate **6b**. Yellow solid. HRMS (ESI) *m/z* 497.2064 [M+H]⁺, Calcd. for 497.2036.

5.1.13.

4-(((2-(tert-butylamino)-6-methoxy-4-(4-nitrophenoxy)quinolin-7-yl)oxy)-*N*-isopropylpiperidine-1-carboxamide (**25**). To a solution of quinoline *N*-oxide **24** (9.9 g, 20.0 mmol) and tert-butylamine (12.3 mL, 120.0 mmol) in CH₂Cl₂ at 0 °C was added 4-methylbenzenesulfonic anhydride (16.3 g, 50.0 mmol) in portions while maintaining the reaction temperature at 0-5 °C. The mixture was warmed to room

temperature and stirred for 1 h. The reaction mixture was quenched with NaHCO₃ aqueous solution (30 mL). The organic layer was separated, concentrated and the crude product was purified by silica gel column chromatography to afford title intermediate as light yellow solid, yield: 62.1%. HRMS (ESI) m/z 552.2870 [M+H]⁺, Calcd. For 552.2822.

5.1.14.

4-((2-(*tert*-butylamino)-4-(4-(3-(2-(2,6-difluorophenyl)-4-oxothiazolidin-3-yl)ureido)phenoxy)-6-methoxyquinolin-7-yl)oxy)-*N*-isopropylpiperidine-1-carboxamide (**30**). Prepared following the synthetic procedure of **11k**. White solid, yield: 36.1%. HRMS (ESI) m/z 778.3244 [M+H]⁺, Calcd. For 778.3198.

5.1.15.

4-((2-amino-4-(4-(3-(2-(2,6-difluorophenyl)-4-oxothiazolidin-3-yl)ureido)phenoxy)-6-methoxyquinolin-7-yl)oxy)-*N*-isopropylpiperidine-1-carboxamide (**31**). To a suspension of **30** (0.39 g, 0.5 mmol) in xylene (3 mL), CF₃COOH (3 mL) was added. The solution was stirred for 5 h at 70 °C. The resulting mixture was concentrated, and the residue was dissolved in CH₂Cl₂ (10 mL) which was basified by 10 % NaOH aqueous solution. CH₂Cl₂ was separated, concentrated in vacuo and the oil was purified by silica gel column chromatography (eluent, CH₂Cl₂: MeOH: Et₃N = 100:5:1 to 100:20:1) to afford the title compound as a white solid, yield: 57.9%, purity: 98.14%. ¹H NMR (400 MHz, DMSO-*d*₆) δ: 9.02 (s, 1H), 8.82 (s, 1H), 7.50-7.54 (m, 4H), 7.48 (s, 1H), 7.16-7.21 (m, 4H), 6.46 (s, 1H), 6.27 (br, 2H), 6.20 (m, 1H), 6.16 (s, 1H), 4.75-4.82 (m, 1H), 3.92 (s, 3H), 3.79-3.84 (m, 2H), 3.72-3.77 (m, 3H), 3.10-3.16 (m, 2H), 1.96-2.01 (m, 2H), 1.53-1.61 (m, 2H), 1.07 (s, 3H), 1.06 (s, 3H). HRMS (ESI) m/z 744.2534 [M+Na]⁺, Calcd. For. 744.2392.

5.1.16. 1-(3-(benzyloxy)-4-methoxyphenyl)ethan-1-one (**32**). To a mixture of 1-(3-hydroxy-4-methoxyphenyl)ethan-1-one (16.6 g, 0.1 mol) and K₂CO₃ (34.5 g, 0.25 mol) in DMF (80 mL), benzyl bromide (18.6 g, 0.11 mol) was added dropwise at room temperature. After stirring for 2 h, the reaction mixture was poured into cold water (400 mL). The suspended solid was obtained by filtration and washed by water. White solid, yield: 89.8%. HRMS (ESI) m/z 257.1212 [M+H]⁺, Calcd. For 257.1178.

5.1.17. 1-(5-(benzyloxy)-4-methoxy-2-nitrophenyl)ethan-1-one (**33**). Fuming HNO₃ (16 mL) was added dropwise at -10 °C to a solution of **32** (25.7 g, 0.1 mol) in CH₂Cl₂ (200 mL). After stirring for 5 h at -10 °C, the solution was poured into ice water (100 mL). The organic layer was washed with saturated sodium bicarbonate (2×50 mL), and brine (50 mL). The organic layers were dried over Na₂SO₄, filtered, and concentrated under vacuum to provide **33** as a yellow solid, yield: 73.6%. HRMS (ESI) m/z 302.1064 [M+H]⁺, Calcd. For 302.1028.

5.1.18. 1-(2-amino-5-(benzyloxy)-4-methoxyphenyl)ethan-1-one (**34**). Powdered iron (0.3 mol) and concentrated HCl (10 drops) was added to a suspension of intermediates **33** (0.1 mol) in 90% EtOH (300 mL). The mixture was refluxed with vigorous agitation for 3 h. The hot mixture was filtered through celites and the filtrate was cooled to 0 °C. The precipitate was filtered and dried to afford **34** as a yellow solid, yield: 78.5%. HRMS (ESI) m/z 272.1329 [M+H]⁺, Calcd. For 272.1287.

5.1.19. 6-(benzyloxy)-7-methoxyquinolin-4-ol (**35**). Intermediate **34** (27.2 g, 0.1 mol)

was dissolved in dry 1,2-dimethoxyethane (250 mL), and MeONa (16.2 g, 0.3 mol) was added in portions. After stirring for 30 min at room temperature, HCOOEt (29.6 g, 0.4 mol) was added dropwise. Cold water (50 mL) was added to the mixture 4 h later, and the resultant solution was acidified by HOAc (pH = 5). The precipitate was filtered, washed by water, and dried to afford **35** as a pale solid, yield: 72.4%. HRMS (ESI) m/z 282.1166 $[M+H]^+$, Calcd. For 282.1130.

5.1.20. 6-(benzyloxy)-4-chloro-7-methoxyquinoline (36). To a suspension of **35** (14.1 g, 0.05 mol) in phosphorus oxychloride (80 mL), 4-dimethylaminopyridine (6.1 g, 0.05 mol) was added at room temperature. The reaction mixture was allowed to warm to 110 °C with stirring for 6 h. The resulting mixture was then concentrated to yield a brown oil. The residue was poured into ice-water (200 mL), and the mixture was basified by Na₂CO₃ (pH = 9). The precipitate was filtered, washed by water, and dried to afford **36** as an off-white solid, yield: 64.7%. HRMS (ESI) m/z 300.0843 $[M+H]^+$, Calcd. For 300.0791.

5.1.21.

4-(((4-(4-(3-(2-(2,6-difluorophenyl)-4-oxothiazolidin-3-yl)ureido)phenoxy)-7-methoxyquinolin-6-yl)oxy)methyl)-N-isopropylpiperidine-1-carboxamide (46). Taking intermediate **36** as starting material, target compound was prepared following the synthetic procedure of **11o**. White solid, yield: 37.2%. ¹H NMR (400 MHz, DMSO-*d*₆) δ : 9.06 (s, 1H), 8.86 (s, 1H), 8.45 (d, J = 5.2 Hz, 1H), 7.47-7.54 (m, 4H), 7.38 (s, 1H), 7.16-7.20 (m, 4H), 6.41 (d, J = 5.2 Hz, 1H), 6.16 (s, 1H), 6.08-6.10 (m, 1H), 4.76-4.82 (m, 1H), 3.98-4.02 (m, 4H), 3.95 (s, 3H), 3.83 (s, 2H), 3.72-3.78 (m, 1H), 2.63-2.70 (m, 2H), 2.00 (br, 1H), 1.75-1.78 (m, 2H), 1.16-1.26 (m, 2H), 1.06 (s, 3H), 1.04 (s, 3H). HRMS (ESI) m/z 743.2563 $[M+Na]^+$, Calcd. For 743.2439.

5.1.22.

4-(((4-(3-(3-(2-(2,6-difluorophenyl)-4-oxothiazolidin-3-yl)ureido)phenoxy)-6-methoxyquinolin-7-yl)oxy)-N-isopropylpiperidine-1-carboxamide (56). Taking 7-(benzyloxy)-4-chloro-6-methoxyquinoline and 3-nitrophenol as starting materials, target compound was prepared following the synthetic procedure of **11k**. White solid, yield: 35.2%. ¹H NMR (400 MHz, DMSO-*d*₆) δ : 9.05 (s, 1H), 8.82 (s, 1H), 8.49 (d, J = 5.2 Hz, 1H), 7.47-7.51 (m, 4H), 7.37-7.41 (m, 2H), 7.25-7.27 (m, 1H), 7.14-7.17 (m, 2H), 6.87-6.89 (m, 1H), 6.52 (d, J = 5.2 Hz, 1H), 6.21-6.23 (m, 1H), 6.11 (s, 1H), 4.78-4.81 (m, 1H), 3.92 (s, 3H), 3.74-3.81 (m, 5H), 3.10-3.15 (m, 2H), 1.98-2.02 (m, 1H), 1.54-1.61 (m, 2H), 1.07 (s, 3H), 1.06 (s, 3H); ¹³C NMR (100 MHz, DMSO-*d*₆) δ : 169.7, 164.1, 160.6, 157.3 (2C), 155.1, 154.2, 150.5, 149.3, 149.0, 137.1, 132.1, 131.9, 121.9 (2C), 120.7, 115.7, 115.4, 115.2, 112.9, 112.5, 110.8, 103.4, 100.1, 73.9, 56.7, 56.2, 42.3, 41.5 (2C), 30.7 (2C), 29.6, 23.4 (2C). HRMS (ESI) m/z 729.2412 $[M+Na]^+$, Calcd. For 729.2283.

5.2. MTT assay

Human colon cancer cell HT-29 was obtained from China Infrastructure of Cell Line Resource. The cytotoxic activities of target compounds were evaluated with HT-29 cells by the standard MTT assay, with Cabozantinib and Regorafenib as positive control. All samples consisted of three replicates. Detailed operation could be found in our previous research [26].

5.3. Mobility shift assay of tyrosine kinases *in vitro*

The selected compound **11k** was tested for its inhibitory activity against c-Met, Ron, c-Kit, PDGFR α , BRAF, IGF-1R, c-Src and AXL through the mobility shift assay. Detailed operation could be found in our previous research [26].

5.4. IncuCyte studies [26,39]

Human normal colorectal mucosa epithelial cell FHC was obtained from Beijing Beina Chuanglian Biotechnology Institute. A total of 5×10^3 HT-29 and FHC cells grown in 100 μ L Dulbecco's Modified Eagle Media (DMEM) with serum (10% FBS) were seeded in 96-well plates respectively and incubated in a tissue culture incubator at 37 °C and 5% CO₂ in a Live-Cell Imaging Analysis System (Essen BioScience). To analyze the cytotoxicity, the DNA fluorescent probe YOYO-1 iodide in a solution of DMSO was added. For apoptosis studies, the CellEvent[®] Caspase 3/7 Green ReadyProbes[®] reagent (Thermo Fisher Scientific; R37111) was added. Confluency was measured by averaging the percentage of area that the cells occupied from three images of a given well every two hours for 72 hours. The cells were cultured for 24 h, and different concentration of compound **11k** and Regorafenib were added. Assay was performed according to the manufacturer's protocol. All samples consisted of three replicates. Green fluorescent signals were measured, and green-fluorescent cells were counted as dead cells and apoptotic cells, respectively.

5.5. Cell-Cycle Assay

HT-29 cells were treated with compound **11k** and Regorafenib at gradient increase from 0.3 to 3.0 μ g/mL for 48 h. Cells were washed with PBS for twice, fixed with 70% cold ethanol at 4 °C overnight. The cells were stained with propidium iodide for 30 min at room temperature in the dark. Cell-cycle analyses were made with a BD Accuri C6 (Becton Dickinson, Franklin Lakes, NJ, USA) and the data was analyzed using FlowJo7.6.1 Software.

5.6. Molecular docking study

All preparation and docking study were performed with Molecular Operating Environment 2018.01 (MOE, Chemical Computing Group ULC, Montreal, QC, Canada) using default settings. The c-Met receptor structure was prepared (protonation, modeling of missing elements) from the original PDB files (PDB ID: 3LQ8) using Quickprepare, and the strength of receptor was 5000. The binding site was defined within 5.0 Å of the cocrystallized ligands coordinates. The docking forcefield was Amber10: EHT. Ligand conformations were placed in the site with the Triangle Matcher method and ranked using the London dG scoring function.

Acknowledgements

This work was supported by the National Natural Science Foundation of China (No. 21562053 and No. 81960627).

References

- [1] E. Zwick, J. Bange, A. Ullrich. Receptor tyrosine kinases as targets for anticancer drugs, *Trends Mol. Med.* 8 (2002) 17–23. [https://doi.org/10.1016/S1471-4914\(01\)02217-1](https://doi.org/10.1016/S1471-4914(01)02217-1).

- [2] T. Hunter. Tyrosine phosphorylation: thirty years and counting, *Curr. Opin. Cell Biol.* 21 (2009) 140–146. <https://doi.org/10.1016/j.ceb.2009.01.028>.
- [3] S. R. Hubbard, T. W. Miller. Receptor tyrosine kinases: mechanisms of activation and signaling, *Curr. Opin. Cell Biol.* 19 (2007) 117–123. <https://doi.org/10.1016/j.ceb.2007.02.010>.
- [4] P. K. Parikh, M. D. Ghate. Recent advances in the discovery of small molecule c-Met Kinase inhibitors, *Eur. J. Med. Chem.* 143 (2018) 1103–1138. <https://doi.org/10.1016/j.ejmech.2017.08.044>.
- [5] L. Trusolino, A. Bertotti, P.M. Comoglio. MET signalling: principles and functions in development, organ regeneration and cancer, *Nat. Rev. Mol. Cell Biol.* 11 (2010) 834–848. <https://doi.org/10.1038/nrm3012>.
- [6] H. Oliveres, E. Pineda, J. Maurel. MET inhibitors in cancer: pitfalls and challenges, *Expert Opin. Inv. Drug.* 29 (2020) 73–85. <https://doi.org/10.1080/13543784.2020.1699532>.
- [7] K. H. Jung, B. H. Park, S. S. Hong. Progress in Cancer Therapy Targeting c-Met Signaling Pathway, *Arch. Pharm. Res.* 35 (2012) 595–604. <https://doi.org/10.1007/s12272-012-0402-6>.
- [8] L. Jia, X. Yang, W. Tain, *et al.* Increased Expression of c-Met is Associated with Chemotherapy-Resistant Breast Cancer and Poor Clinical Outcome, *Med Sci Monit* 24 (2018) 8239–8249. <https://doi.org/10.12659/MSM.913514>.
- [9] I. Cañadas, F. Rojo, M. Arumí-Uría, *et al.* C-MET as a new therapeutic target for the development of novel anticancer drugs, *Clin Transl Oncol* 12 (2010) 253–260. <https://doi.org/10.1007/s12094-010-0501-0>.
- [10] P. Marona, J. Górka, J. Kotlinowski, *et al.* C-Met as a Key Factor Responsible for Sustaining Undifferentiated Phenotype and Therapy Resistance in Renal Carcinomas, *Cells* 8 (2019) 272–288. <https://doi.org/10.3390/cells8030272>.
- [11] N. Faham, A. L. Welm. RON Signaling Is a Key Mediator of Tumor Progression in Many Human Cancers, *Cold Spring Harb Symp Quant Biol.* 81 (2016) 177–188. <https://doi.org/10.1101/sqb.2016.81.031377>.
- [12] N. M. Benight, S. E. Waltz. Ron receptor tyrosine kinase signaling as a therapeutic target, *Expert Opin. Ther. Targets* 16 (2012) 921–931. <https://doi.org/10.1517/14728222.2012.710200>.
- [13] E. R. Camp, A. Yang, M. J. Gray, *et al.* Tyrosine kinase receptor RON in human pancreatic cancer: expression, function, and validation as a target. *Cancer* 109 (2007) 1030–1039. <https://doi.org/10.1002/cncr.22490>.
- [14] M. H. Wang, D. Wang, Y. Q. Chen. Oncogenic and invasive potentials of human macrophage-stimulating protein receptor, the RON receptor tyrosine kinase. *Carcinogenesis* 24 (2003) 1291–1300. <https://doi.org/10.1093/carcin/bgg089>.
- [15] A. Danilkovitch-Miagkova. Oncogenic signaling pathways activated by RON receptor tyrosine kinase. *Curr. Cancer Drug Targets* 3 (2003) 31–40. <https://doi.org/10.2174/1568009033333745>.
- [16] B. Yin, Z. Liu, Y. Wang, *et al.* RON and c-Met facilitate metastasis through the ERK signaling pathway in prostate cancer cells, *Oncol Rep.* 37 (2017) 3209–3218. <https://doi.org/10.3892/or.2017.5585>.

- [17] S. A. Kim, K. H. Lee, D. H. Lee, *et al.* Receptor tyrosine kinase, RON, promotes tumor progression by regulating EMT and the MAPK signaling pathway in human oral squamous cell carcinoma, *Int. J. Oncol.* 55 (2019) 513–526. <https://doi.org/10.3892/ijo.2019.4836>.
- [18] O. Zarei, S. Benvenuti, F. Ustun-Alkan, *et al.* Strategies of targeting the extracellular domain of RON tyrosine kinase receptor for cancer therapy and drug delivery, *J. Cancer Res. Clin. Oncol.* 142 (2016) 2429–2446. <https://doi.org/10.1007/s00432-016-2214-4>.
- [19] C. T. Cheng, Y. Y. Chen, R. C. Wu, *et al.* MET/RON dual inhibitor, BMS-777607, suppresses cholangiocarcinoma cell growth, and MET/RON upregulation indicates worse prognosis for intrahepatic cholangiocarcinoma patients, *Oncol. Rep.* 40 (2018) 1411–1421. <https://doi.org/10.3892/or.2018.6543>.
- [20] G. M. Schroeder, Y. An, Z. W. Cai, *et al.* Discovery of *N*-(4-(2-Amino-3-chloropyridin-4-yloxy)-3-fluorophenyl)-4-ethoxy-1-(4-fluorophenyl)-2-oxo-1,2-dihydropyridine-3-carboxamide (BMS-777607), a Selective and Orally Efficacious Inhibitor of the Met Kinase Superfamily, *J. Med. Chem.* 52 (2009) 1251–1254. <https://doi.org/10.1021/jm801586s>.
- [21] J. J. Cui, M. Tran-Dubé, H. Shen, *et al.* Structure Based Drug Design of Crizotinib (PF-02341066), a Potent and Selective Dual Inhibitor of Mesenchymal Epithelial Transition Factor (c-MET) Kinase and Anaplastic Lymphoma Kinase (ALK), *J. Med. Chem.* 54 (2011) 6342–6363. <https://doi.org/10.1021/jm2007613>.
- [22] P. C. Lv, Y. S. Yang, Z. C. Wang. Recent Progress in the Development of Small Molecule c-Met Inhibitors, *Curr. Top. Med. Chem.* 19 (2019) 1276–1288. <https://doi.org/10.2174/1568026619666190712205353>.
- [23] A. B. Northrup, M. H. Katcher, M. D. Altman, *et al.* Discovery of 1-[3-(1-Methyl-1H-pyrazol-4-yl)-5-oxo-5H-benzo[4,5]cyclohepta[1,2-b]pyridin-7-yl]-N-(pyridin-2-ylmethyl)methanesulfonamide (MK-8033): A Specific c-Met/Ron Dual Kinase Inhibitor with Preferential Affinity for the Activated State of c-Met, *J. Med. Chem.* 56 (2013) 2294–2310. <https://doi.org/10.1021/jm301619u>.
- [24] I. Kawada, R. Hasina, Q. Arif, *et al.* Dramatic Antitumor Effects of the Dual MET/RON Small-Molecule Inhibitor LY2801653 in Non-Small Cell Lung Cancer, *Cancer Res.* 74 (2014) 884–895. <https://doi.org/10.1158/0008-5472.CAN-12-3583>.
- [25] S. Baltschukat, B. S. Engstler, A. Huang, *et al.* Capmatinib (INC280) Is Active Against Models of Non-Small Cell Lung Cancer and Other Cancer Types with Defined Mechanisms of MET Activation, *Clin Cancer Res.* 25 (2019) 3164–3175. <https://doi.org/10.1158/1078-0432.CCR-18-2814>.
- [26] B. Qi, Y. Yang, G. Gong, *et al.* Discovery of *N*¹-(4-((7-(3-(4-ethylpiperazin-1-yl)propoxy)-6-methoxyquinolin-4-yl)oxy)-3,5-difluorophenyl)-*N*³-(2-(2,6-difluorophenyl)-4-oxothiazolidin-3-yl)urea as a multi-tyrosine kinase inhibitor for drug-sensitive and drug-resistant cancers

- treatment, *Eur. J. Med. Chem.* 163 (2019) 10–27. <https://doi.org/10.1016/j.ejmech.2018.11.057>.
- [27] I. Szabadkai, R. Torka, R. Garamvölgyi, *et al.* Discovery of *N*-[4-(Quinolin-4-yloxy)phenyl]benzenesulfonamides as Novel AXL Kinase Inhibitors, *J. Med. Chem.* 61 (2018) 6277–6292. <https://doi.org/10.1021/acs.jmedchem.8b00672>.
- [28] L. Pisani, R. M. Lacobazzi, M. Catto, *et al.* Investigating alkyl nitrates as nitric oxide releasing precursors of multitarget acetylcholinesterase-monoamine oxidase B inhibitors, *Eur. J. Med. Chem.* 161 (2019) 292–309. <https://doi.org/10.1016/j.ejmech.2018.10.016>.
- [29] C. Riemer, E. Borroni, B. Levet-Trafit, *et al.* Influence of the 5-HT₆ Receptor on Acetylcholine Release in the Cortex: Pharmacological Characterization of 4-(2-Bromo-6-pyrrolidin-1-ylpyridine-4-sulfonyl)phenylamine, a Potent and Selective 5-HT₆ Receptor Antagonist, *J. Med. Chem.* 46 (2003) 1273–1276. <https://doi.org/10.1021/jm021085c>.
- [30] J. Yin, B. Xiang, M. A. Huffman, *et al.* A General and Efficient 2-Amination of Pyridines and Quinolines, *J. Org. Chem.* 72 (2007) 4554–4557. <https://doi.org/10.1021/jo070189y>.
- [31] B. Qi, Y. Yang, H. He, *et al.* Identification of novel *N*¹-(2-aryl-1,3-thiazolidin-4-one)-*N*³-aryl ureas showing potent multi-tyrosine kinase inhibitory activities, *Eur. J. Med. Chem.* 146 (2018) 368–380. <https://doi.org/10.1016/j.ejmech.2018.01.061>.
- [32] T. P. Forsyth, M. B. Mac, J. W. Leahy, *et al.* Preparation of quinolines as modulators of c-Met, KDR, c-Kit, flt-3, and flt-4 kinases, WO2006108059A1, 2006-10-12.
- [33] Y. L. Park, G. H. Lee, K. Y. Kim, *et al.* Expression of RON in colorectal cancer and its relationships with tumor cell behavior and prognosis, *Tumori* 98 (2012) 652–662. <https://doi.org/10.1177/030089161209800517>.
- [34] S. M. Parizadeh, R. J. Esfehiani, D. Fazilat-Panah, *et al.* The Potential Therapeutic and Prognostic Impacts of the c-MET/HGF Signaling Pathway in Colorectal Cancer, *IUBMB Life* 71 (2019) 802–811. <https://doi.org/10.1002/iub.2063>.
- [35] J. Yao, X. Li, L. Yan, *et al.* Role of HGF/c-Met in the treatment of colorectal cancer with liver metastasis, *J Biochem Mol Toxicol.* 33 (2019) e22316. <https://doi.org/10.1002/jbt.22316>.
- [36] J. Li, J. Yuan. Caspases in apoptosis and beyond, *Oncogene* 27 (2008) 6194–6206. <https://doi.org/10.1038/onc.2008.297>.
- [37] K. Ito, Z. Maruyama, A. Sakai, *et al.* Overexpression of Cdk6 and Cnd1 in chondrocytes inhibited chondrocyte maturation and caused p53-dependent apoptosis without enhancing proliferation, *Oncogene* 33 (2014) 1862–1871. <https://doi.org/10.1038/onc.2013.130>.
- [38] M. S. Jeong, J.H. Jung, H. Lee, *et al.* Methyloleanolate Induces Apoptotic And Autophagic Cell Death Via Reactive Oxygen Species Generation And c-Jun N-terminal Kinase Phosphorylation, *Onco Targets Ther.* 12 (2019) 8621–8635.

<https://doi.org/10.2147/OTT.S211904>.

- [39] B. Qi, X. Xu, Y. Yang, *et al.* Discovery of thiazolidin-4-one urea analogues as novel multikinase inhibitors that potently inhibit FLT3 and VEGFR2, *Bio. Med. Chem.* 27 (2019) 2127–2139. <https://doi.org/10.1016/j.bmc.2019.03.049>.

Journal Pre-proof

Identification of Novel Quinoline Analogues Bearing Thiazolidinones as Potent Kinase Inhibitors for the Treatment of Colorectal Cancer

Yuting Zhou, Xingwei Xu, Fei Wang, Huan He, Guowei Gong, Li Xiong, Baohui Qi^{*1}

Department of Bioengineering, Zhuhai Campus of Zunyi Medical University, Zhuhai, 519041,
Guangdong Province, China

Research highlights

- ▶ Novel quinoline analogues bearing thiazolidinones were designed and synthesized.
- ▶ **11k** possessing potent inhibitory activity against multi-kinases was identified.
- ▶ Antitumor activity on HT-29 of **11k** was 9.3-fold more potent than that of Regorafenib.
- ▶ Excellent antiproliferation, cytotoxicity, and induction of apoptosis were confirmed.
- ▶ The toxicity to FHC cells of **11k** was much lower than that of Regorafenib.

*Corresponding authors.
E-mail address: bhqi@zmu.gd.cn.

Declaration of interests

The authors declare that we have no known competing financial interests or personal relationships that could have appeared to influence the work reported in this manuscript entitled “Identification of Novel Quinoline Analogues Bearing Thiazolidinones as Potent Kinase Inhibitors for the Treatment of Colorectal Cancer”.

Journal Pre-proof